

## Electronic Supplementary Information

### Defect-Engineering a Metal-Organic Framework for CO<sub>2</sub> Fixation in the Synthesis of Bioactive Oxazolidinones

Aasif Helal,<sup>a,\*</sup> Kyle E. Cordova,<sup>b</sup> Md. Eyasin Arafat,<sup>a</sup> Muhammad Usman,<sup>a</sup> and Zain  
H. Yamani<sup>a</sup>

<sup>a</sup>Center of Research Excellence in Nanotechnology (CENT), King Fahd University of  
Petroleum and Minerals (KFUPM), Dhahran 31261, Saudi Arabia

<sup>b</sup>Materials Discovery Research Unit, Reticular Foundry, Royal Scientific Society,  
Amman 11941, Jordan

#### Table of Contents

<b>Section S1</b>	<i>Experimental section</i>	S2-5
<b>Section S2</b>	<i>Characterization of UiO-66 and UiO-66 analogues</i>	S6-15
<b>Section S3</b>	<i><sup>1</sup>H and <sup>13</sup>C NMR of oxazolidinones</i>	S16-20
<b>Section S4</b>	<i><sup>1</sup>H and <sup>13</sup>C NMR spectra of oxazolidinones</i>	S21-33
<b>Section S5</b>	<i>Synthesis of the intermediates for the catalytic reaction</i>	S34-36
<b>Section S6</b>	<i>Recycling and regeneration of the catalyst UiO-66-40</i>	S37-38
<b>Section S7</b>	<i>References</i>	S39

## Section S1: Experimental section

### Chemicals used in this work

Terephthalic acid (98% purity) (TPA), Zirconium tetrachloride (99.99% purity) ( $\text{ZrCl}_4$ ), 4-(Aminomethyl) benzoic acid (97% purity) (AMBA), methanol (99.9% purity), *N,N*-dimethylformamide (DMF; 99.8% purity), dichloromethane (99.8% extra dry grade), Aniline (99%) with all the other aromatic amines, and propylene oxide (99%) with all the other epoxides were purchased from Sigma Aldrich Corporation. NMR solvents: Chloroform-*d* ( $\text{CDCl}_3$ ; 99.9% purity) and dimethyl sulfoxide-*d*<sub>6</sub> ( $\text{DMSO-}d_6$ ; 99.9% purity) were purchased from Cambridge Isotope. All chemicals were used without further purification. Water used in this work was doubly distilled and filtered through a Millipore membrane.

### Instrumentation

$^1\text{H}$  and  $^{13}\text{C}$  NMR spectra were recorded on a Bruker AM-400 spectrometer using TMS as the internal standard. Powder X-ray diffraction (PXRD) patterns of the samples were recorded using a Rigaku MiniFlex diffractometer, which was equipped with  $\text{Cu K}\alpha$  radiation. The data were acquired over the  $2\theta$  range of  $5^\circ$  and  $40^\circ$ . The FT-IR spectra of the KFUPM-3 were obtained using a Nicolet 6700 Thermo Scientific instrument in the range of  $400\text{-}4000\text{ cm}^{-1}$ , using KBr. Thermogravimetric analysis (TGA) was conducted using a TA Q500 with the sample held in a platinum pan under airflow. The BET surface area of the MOF and its derivatives were calculated by using Micromeritics ASAP 2020 instrument. A liquid nitrogen bath was used for the measurements at 77 K.  $\text{CO}_2$  sorption isotherms were measured on an Autosorb iQ2 volumetric gas adsorption analyzer. The measurement temperatures at 273 and 298 K were controlled with a water circulator.

## Synthesis of MOFs

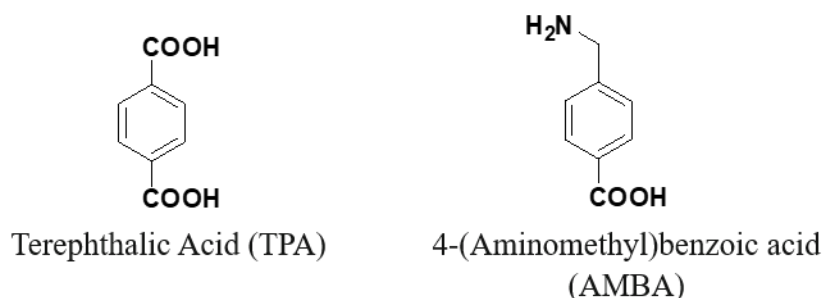


**Figure S1.** Structure of the linkers used in this study.

The MOFs were prepared solvothermally with slight modification of a reported method.<sup>1</sup> The synthesis was carried out with a molar ratio of  $\text{ZrCl}_4$ :TPA:AMBA (1:1:1) in a mixed solvent of DMF (40 mL) and acetic acid (2.8 mL). The reaction mixtures were mixed according to Table S1 to maintain the ratio of the linker modified defects. Then the contents were transferred to a Teflon-lined autoclave and heated at 120 °C for 24 hours. The resulting solid products obtained were cooled, washed three times with DMF (5 mL) using a centrifuge (10,000 rpm for 15 min), and then sequentially immersed in methanol (5 mL three times per day) for three 24 h periods. Finally, each of the product was activated by removing the solvent under vacuum for 24 h at 100 °C. The obtained MOFs are denoted as UiO-66-X, where X is the percentage of AMBA found in the structure (X = 10, 20, 30, 40%). Elemental analysis is as follows:

**UiO-66-10:** Calcd for  $\text{Zr}_6\text{C}_{54}\text{H}_{48.4}\text{N}_{2.6}\text{O}_{34.8} = \text{Zr}_6\text{O}_4(\text{OH})_4(\text{TPA})_{5.4}(\text{AMBA})_{0.6} \cdot (\text{H}_2\text{O})_2 \cdot (\text{DMF})_2$ : C, 35.29; H, 2.65; N, 1.98%. Found: C, 35.74; H, 2.59; N, 1.99%.

**UiO-66-20:** Calcd for  $\text{Zr}_6\text{C}_{54}\text{H}_{50.8}\text{N}_{3.2}\text{O}_{33.6} = \text{Zr}_6\text{O}_4(\text{OH})_4(\text{TPA})_{4.8}(\text{AMBA})_{1.2} \cdot (\text{H}_2\text{O})_2 \cdot (\text{DMF})_2$ : C, 35.45; H, 2.80; N, 2.45%. Found: C, 35.91; H, 2.74; N, 2.43%.

**UiO-66-30:** Calcd for  $\text{Zr}_6\text{C}_{54}\text{H}_{53.2}\text{N}_{3.8}\text{O}_{32.4} = \text{Zr}_6\text{O}_4(\text{OH})_4(\text{TPA})_{4.2}(\text{AMBA})_{1.8} \cdot (\text{H}_2\text{O})_2 \cdot (\text{DMF})_2$ : C, 35.61; H, 2.94; N, 2.92%. Found: C, 36.07; H, 2.88; N, 2.89%.

**UiO-66-40:** Calcd for  $\text{Zr}_6\text{C}_{54}\text{H}_{55.6}\text{N}_{4.4}\text{O}_{31.2} = \text{Zr}_6\text{O}_4(\text{OH})_4(\text{TPA})_{3.6}(\text{AMBA})_{2.4} \cdot (\text{H}_2\text{O})_2 \cdot (\text{DMF})_2$ : C, 35.78; H, 3.09; N, 3.40%. Found: C, 36.14; H, 3.01; N, 3.45%.

**Table S1.** Molar Compositions of Major Precursors for the Syntheses of MOFs from TPA and AMBA and the Yields of MOFs

MOF <sup>a</sup>	ZrCl <sub>4</sub> (mmole)/ Wt (mg)	TPA(mmole)/ Wt (mg)	AMBA(mmole)/ Wt (mg)	Yield (%) <sup>b</sup>
UiO-66	1/233	1/167	0	80
UiO-66- 10	1/233	0.9/150	0.16/24	80
UiO-66- 20	1/233	0.8/134	0.27/41	75
UiO-66- 30	1/233	0.7/117	0.37/56	74
UiO-66- 40	1/233	0.6/100	0.45/68	72

---

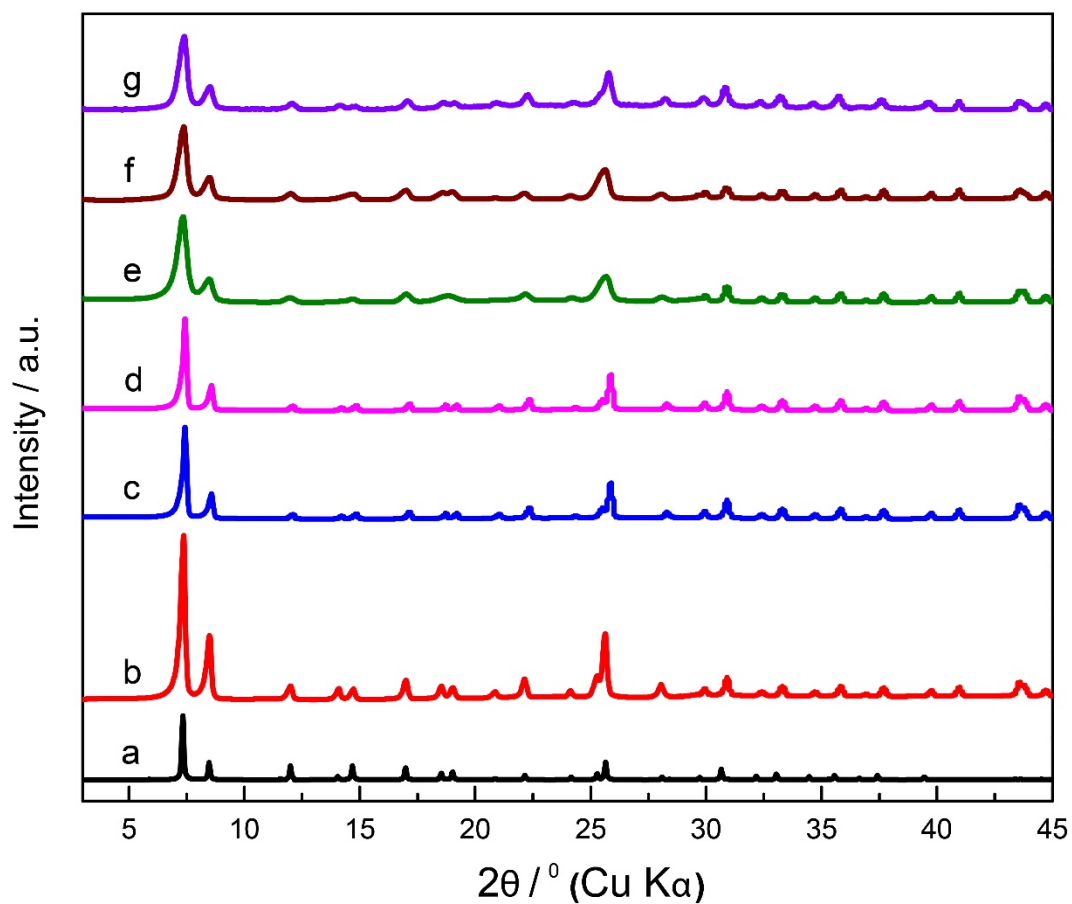
<sup>a</sup>Synthesis temperature: 120 °C, time: 24 h <sup>b</sup>Based on Zr

---

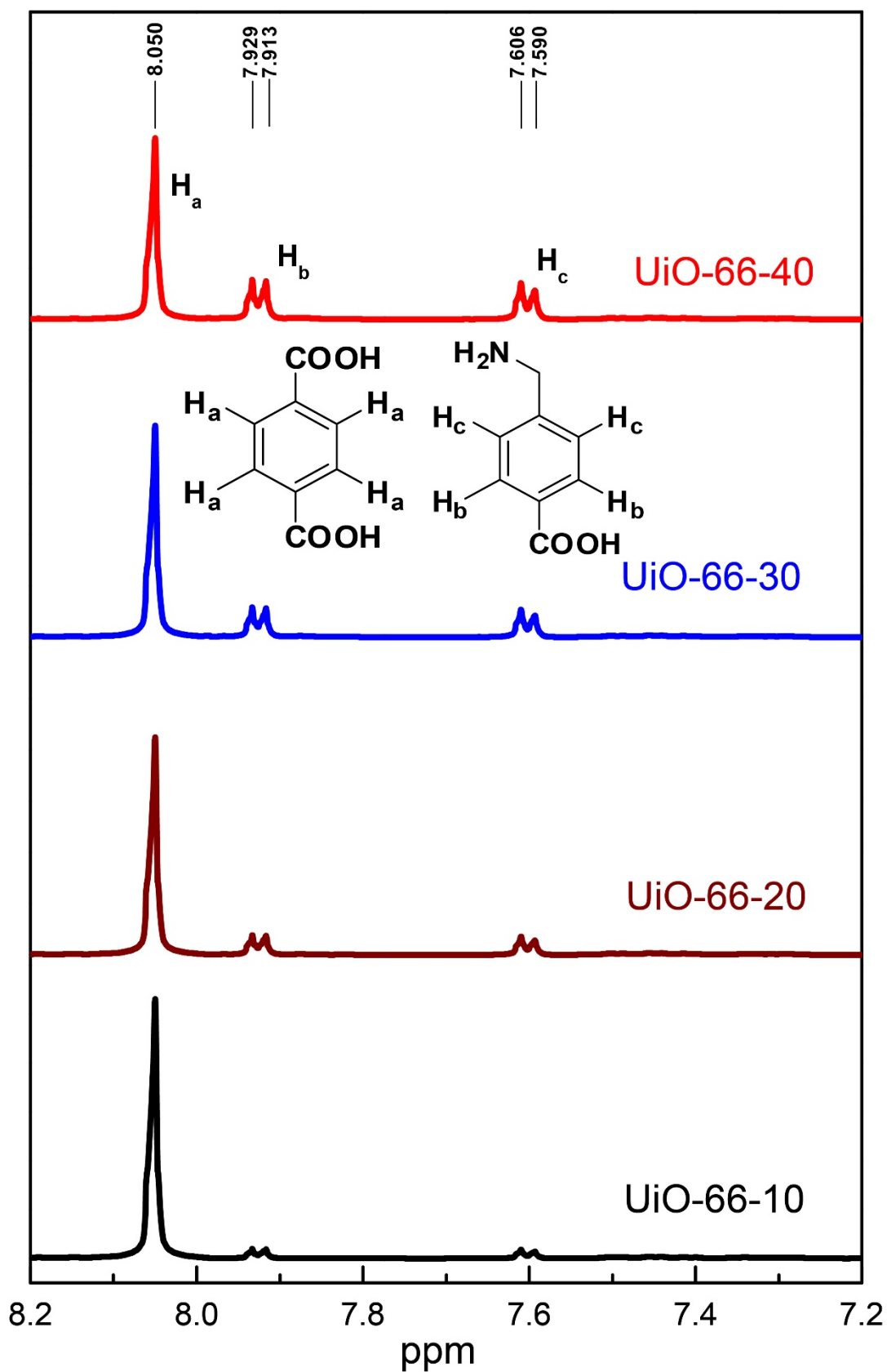
## **General Procedure for Synthesis of Oxazolidinones from Aromatic Amines, Epoxides, and CO<sub>2</sub>**

In a typical reaction, UiO-66 catalyst (70 mg), epoxide (6.0 mmol), and aromatic amine (2.0 mmol) were introduced into a 10 mL Schlenk flask. The flask was equipped with a balloon of CO<sub>2</sub>, and the reaction mixture was stirred on a magnetic stirrer at 85 °C for 12 h. Upon completion of the reaction, the mixture was cooled to room temperature. The catalyst was separated by centrifugation with ethyl acetate three times. The combined ethyl acetate layer was concentrated, and the product was isolated by column chromatography (ethyl acetate/hexane). The product was characterized by <sup>1</sup>H and <sup>13</sup>C NMR spectra and the identities of the oxazolidinones were confirmed by comparison with literature data.<sup>2,3</sup>

## Section S2: Characterization of UiO-66 and UiO-66 analogues



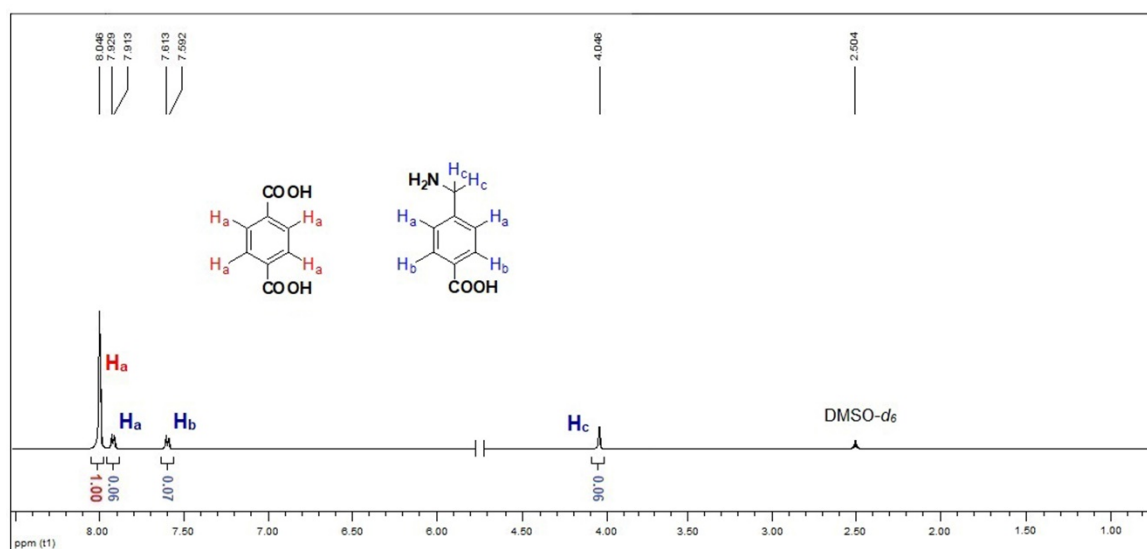
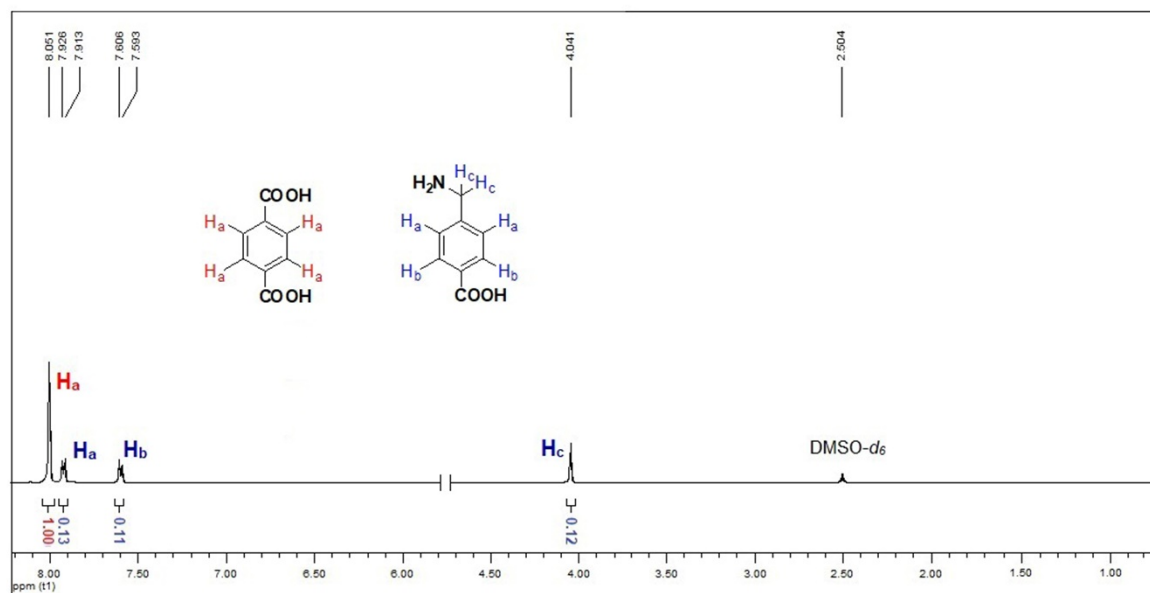
**Figure S2.** PXRD patterns of (a) theoretical UiO-66 (simulated from CIF file), (b) UiO-66, (c) UiO-66-10 (input 16 mol%), (d) UiO-66-20 (input 27 mol%), (e) UiO-66-30 (input 37 mol%), (f) UiO-66-40 (input 45 mol%) and (g) UiO-66-40 after the activation for the isotherm measurements.



**Figure S3.** Digestion  $^1\text{H}$  NMR of UiO-66-10, UiO-66-20, UiO-66-30, and UiO-66-40 showing the presence of both the linkers (TPA and AMBA) in different ratios.

**Table S2.** Input and output ratio of the linkers obtained from the digestion NMR

MOF	Ratio of linkers TPA : AMBA input in mmole.	Ratio of linkers TPA : AMBA output from NMR digestion.
UiO-66-10	1:0.18	1:0.11
UiO-66-20	1:0.34	1:0.25
UiO-66-30	1:0.53	1:0.44
UiO-66-40	1:0.75	1:0.64

**Figure S4:** Digestion <sup>1</sup>H NMR of UiO-66-10 indicating the ratio of the two linkers.**Figure S5:** Digestion <sup>1</sup>H NMR of UiO-66-20 indicating the ratio of the two linkers.



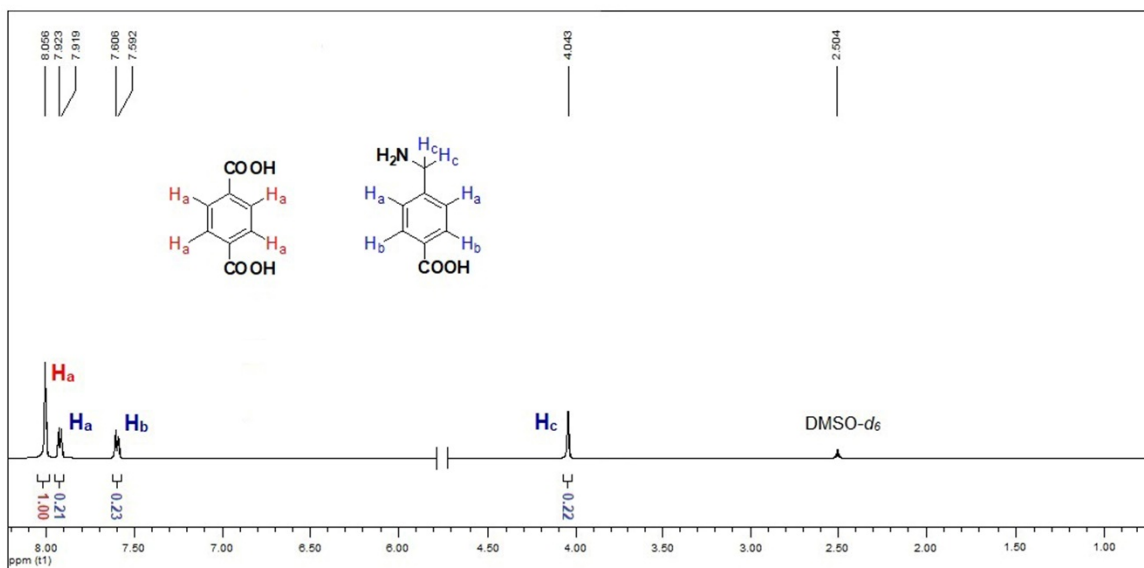


**Figure S6:** Digestion  $^1\text{H}$  NMR of UiO-66-30 indicating the ratio of the two linkers.

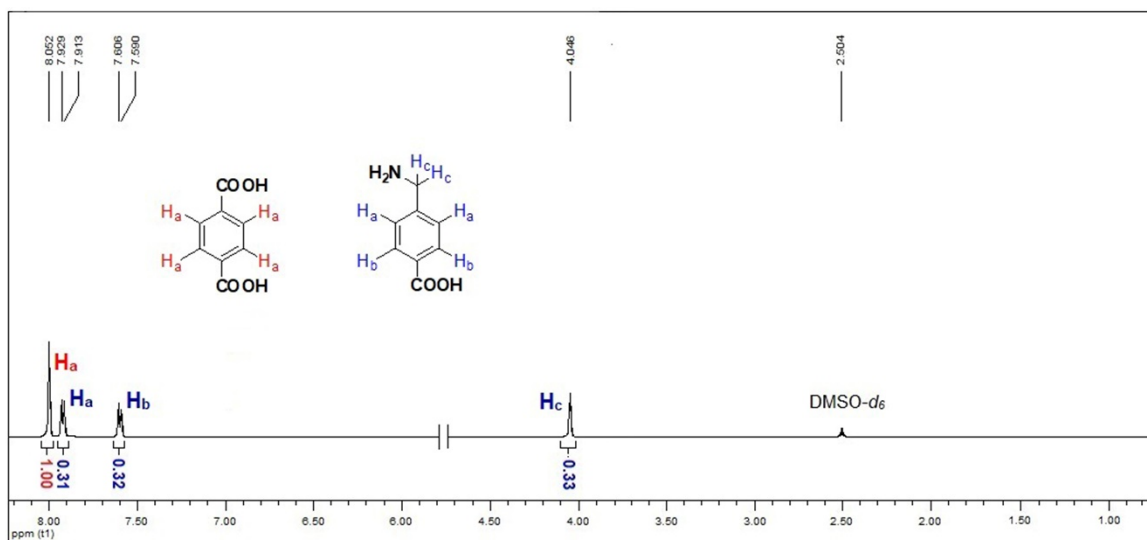


**Figure S7:** Digestion  $^1\text{H}$  NMR of UiO-66-40 indicating the ratio of the two linkers.

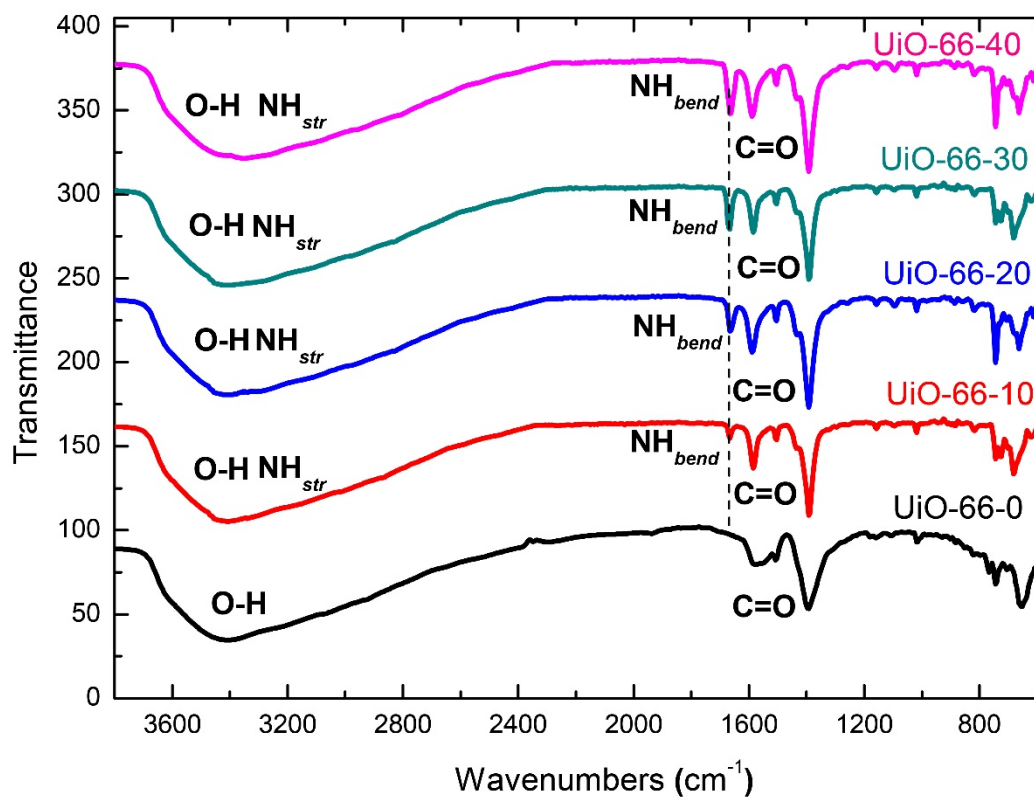


**Figure S8:** FT-IR spectra of UiO-66, UiO-66-10, UiO-66-20, UiO-66-30, and UiO-66-40.

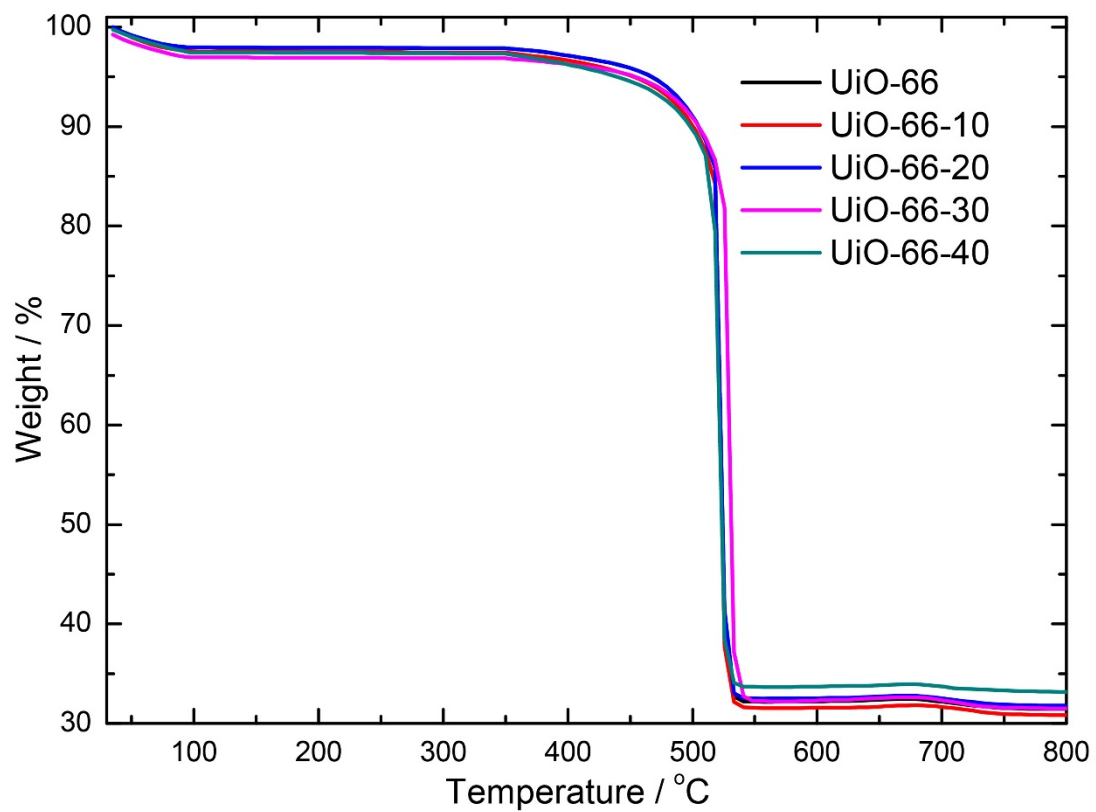


**Figure S9:** Thermal stability of UiO-66, UiO-66-10, UiO-66-20, UiO-66-30, and UiO-66-40.

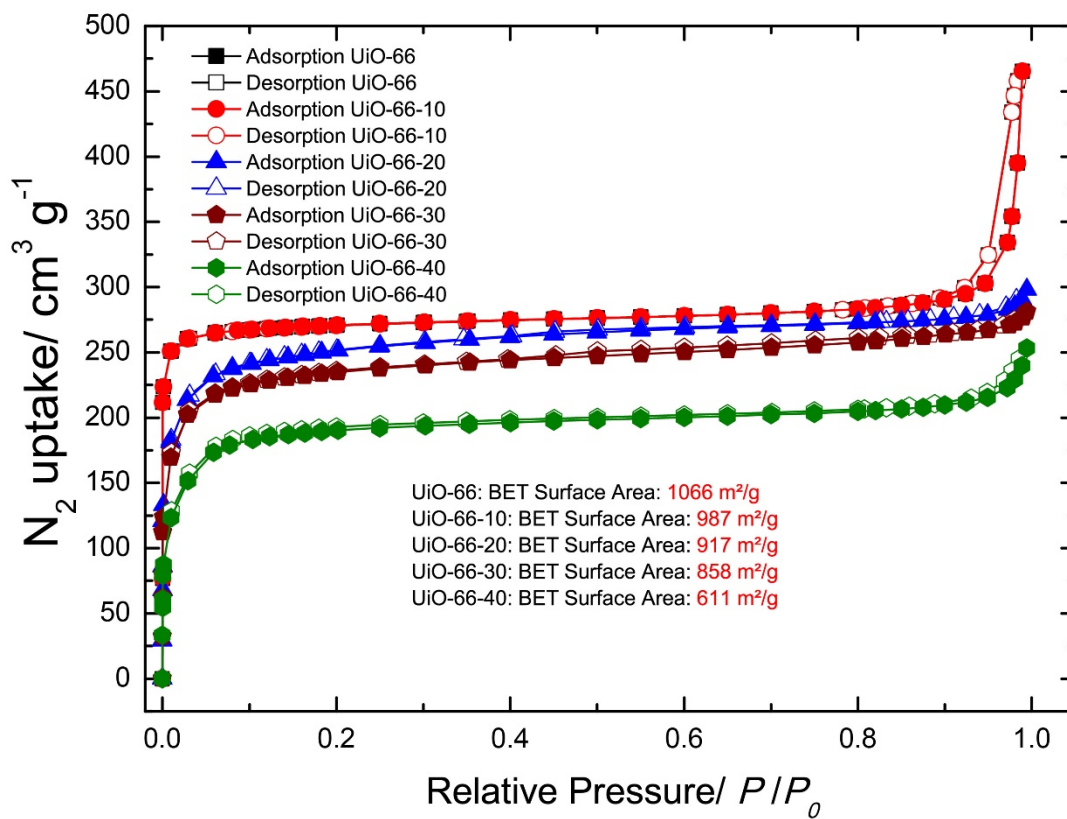


**Figure S10.** N<sub>2</sub> adsorption isotherms of UiO-66, UiO-66-10, UiO-66-20, UiO-66-30, and UiO-66-40. The filled and open circles represent the adsorption and desorption branches, respectively.

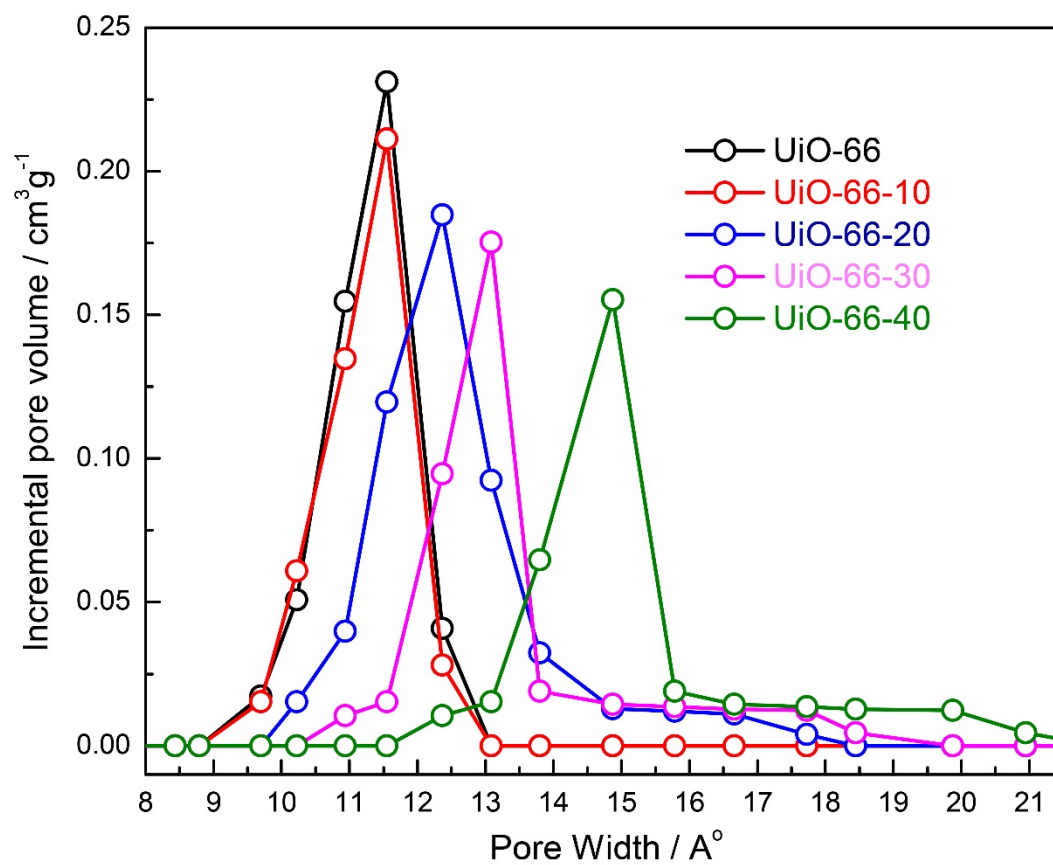


**Figure S11.** DFT pore size distribution plots of UiO-66, UiO-66-10, UiO-66-20, UiO-66-30, and UiO-66-40 at 77 K.

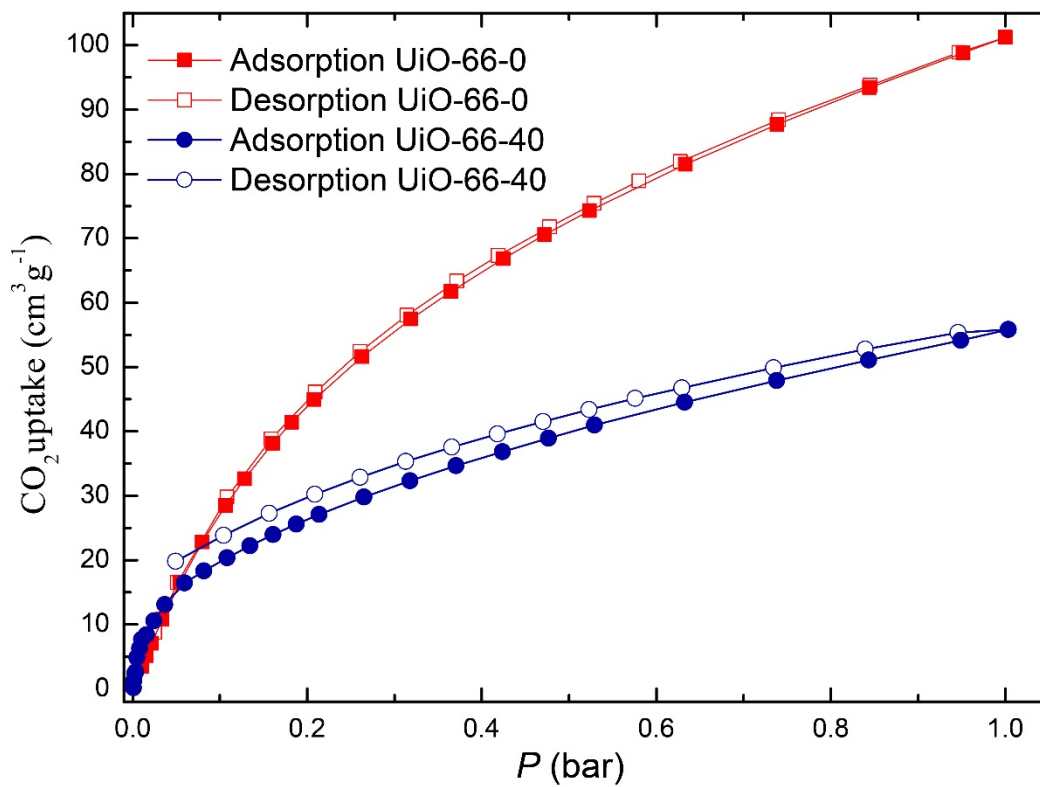


**Figure S12:** CO<sub>2</sub> adsorption isotherms of UiO-66 and UiO-66-40 at 273 K.

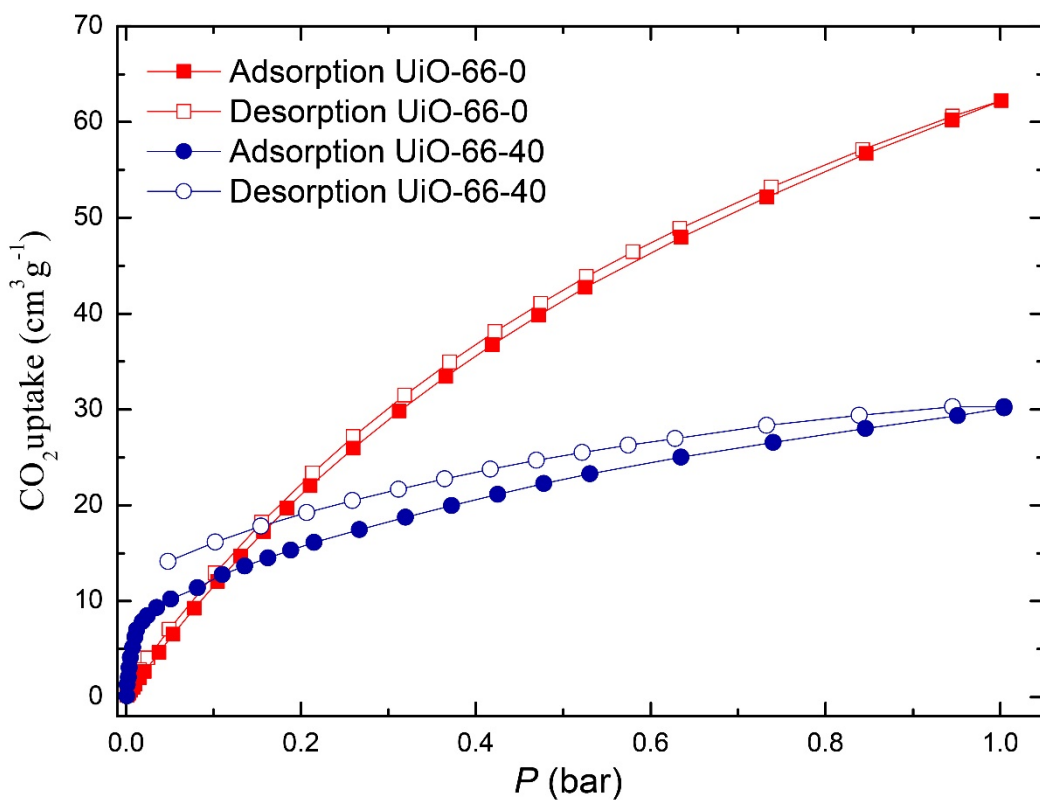


**Figure S13:** CO<sub>2</sub> adsorption isotherms of UiO-66 and UiO-66-40 at 298 K.

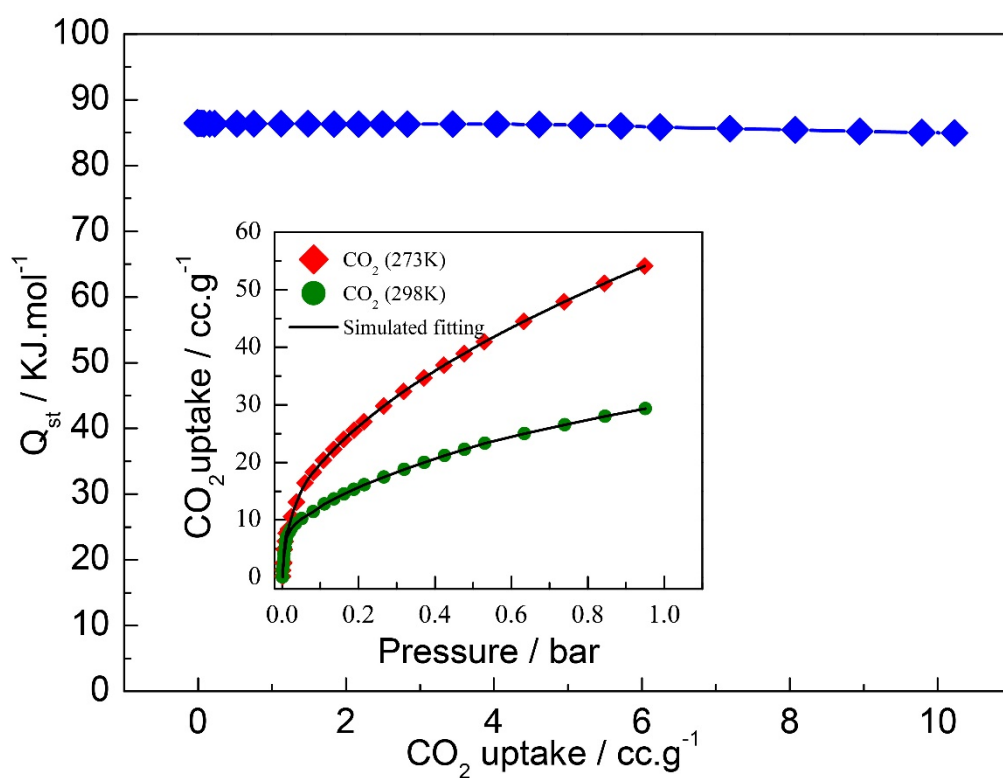
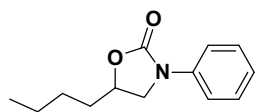


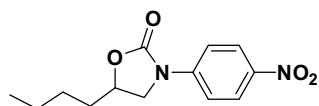
**Figure S14.** Coverage-dependent enthalpy of adsorption ( $Q_{st}$ ) for  $\text{CO}_2$  collected at 273 K and 298 K for UiO-66-40.

### Section S3: <sup>1</sup>H and <sup>13</sup>C NMR of oxazolidinones



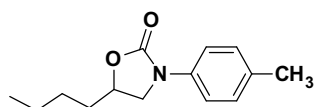
#### Compound C1:

<sup>1</sup>H NMR (400 MHz, CDCl<sub>3</sub>) δ 7.55 (d, *J* = 8.0 Hz, 2H, ArH), 7.38 (t, *J* = 8.0 Hz, 2H, ArH), 7.14 (t, *J* = 7.4 Hz, 2H, ArH), 4.67-4.60 (m, 1H, CH), 4.08 (t, *J* = 8.4 Hz, 1H, CH), 3.66 (t, *J* = 8.0 Hz, 1H, CH), 1.88-1.71 (m, 2H, CH<sub>2</sub>), 1.45-1.41 (m, 4H, CH<sub>2</sub>), 0.96 (t, *J* = 7.2 Hz, 3H, CH<sub>3</sub>). <sup>13</sup>C NMR (400 MHz, CDCl<sub>3</sub>) δ 13.8, 22.3, 26.6, 34.6, 50.4, 73.0, 118.1, 123.8, 128.9, 138.4, 154.9.



#### Compound C2:

<sup>1</sup>H NMR (400 MHz, CDCl<sub>3</sub>) δ 8.07 (d, *J* = 7.2 Hz, 2H, ArH), 6.55 (d, *J* = 7.6 Hz, 2H, ArH), 3.54 (d, *J* = 7.6, 11.6 Hz, 1H, CH), 3.38-3.31 (m, 1H, CH), 3.11 (t, *J* = 6.8 Hz, 1H, CH), 1.44-1.33 (m, 6H, CH<sub>2</sub>), 0.92 (t, *J* = 5.6 Hz, 3H, CH<sub>3</sub>). <sup>13</sup>C NMR (400 MHz, CDCl<sub>3</sub>) δ 13.9, 22.7, 27.6, 32.8, 49.0, 70.3, 111.2, 118.8, 126.4, 137.9, 153.5.

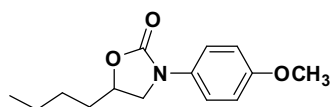


#### Compound C3:

<sup>1</sup>H NMR (400 MHz, CDCl<sub>3</sub>) δ 7.4 (d, *J* = 6.8 Hz, 2H, ArH), 7.16 (d, *J* = 6.8 Hz, 2H, ArH), 4.63-4.58 (m, 1H, CH), 4.04 (t, *J* = 6.8 Hz, 1H, CH), 3.62 (t, *J* = 5.6 Hz, 1H, CH), 2.32 (s, 3H, CH<sub>3</sub>), 1.86-1.70 (m, 2H, CH<sub>2</sub>), 1.44-1.38 (m, 4H, CH<sub>2</sub>), 0.94 (t, *J* = 5.6

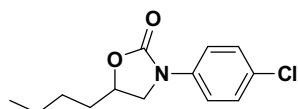


Hz, 3H, CH<sub>3</sub>). <sup>13</sup>C NMR (400 MHz, CDCl<sub>3</sub>) δ 13.9, 20.7, 22.4, 26.6, 34.8, 50.7, 73.1, 118.3, 129.5, 133.6, 135.9, 155.1.



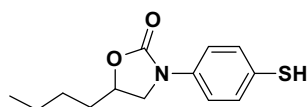
**Compound C4:**

<sup>1</sup>H NMR (400 MHz, CDCl<sub>3</sub>) δ 7.43 (d, *J* = 7.2 Hz, 2H, ArH), 6.9 (d, *J* = 7.2 Hz, 2H, ArH), 4.73-4.68 (m, 1H, CH), 4.53 (t, *J* = 6.4 Hz, 1H, CH), 4.07 (t, *J* = 6.4 Hz, 1H, CH), 3.79 (s, 3H, OCH<sub>3</sub>), 1.85-1.68 (m, 2H, CH<sub>2</sub>) 1.44-1.38 (m, 4H, CH<sub>2</sub>) 0.93 (t, *J* = 5.2 Hz, 3H, CH<sub>3</sub>). <sup>13</sup>C NMR (400 MHz, CDCl<sub>3</sub>) δ 13.7, 22.2, 26.3, 33.5, 50.9, 69.3, 73.0, 114.1, 120.0, 131.5, 155.0, 156.2.



**Compound C5:**

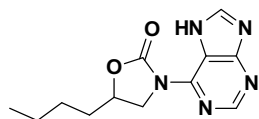
<sup>1</sup>H NMR (400 MHz, CDCl<sub>3</sub>) δ 7.57 (d, *J* = 9.2 Hz, 2H, ArH), 7.42 (d, *J* = 8.8 Hz, 2H, ArH), 4.69-4.62 (m, 1H, CH), 4.12 (t, *J* = 8.6 Hz, 1H, CH), 3.69 (t, *J* = 8.2 Hz, 1H, CH), 1.73-1.67 (m, 2H, CH<sub>2</sub>) 1.35-1.32 (m, 4H, CH<sub>2</sub>) 0.88 (t, *J* = 6.8 Hz, 3H, CH<sub>3</sub>). <sup>13</sup>C NMR (400 MHz, CDCl<sub>3</sub>) δ 13.9, 21.9, 26.2, 33.7, 49.6, 73.1, 119.5, 127.2, 128.7, 137.6, 154.3.



**Compound C6:**

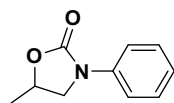
<sup>1</sup>H NMR (400 MHz, CDCl<sub>3</sub>) δ 7.39 (d, *J* = 6.8 Hz, 2H, ArH), 7.27 (d, *J* = 6.8 Hz, 2H, ArH), 4.79-4.74 (m, 1H, CH), 4.55 (t, *J* = 6.4 Hz, 1H, CH), 4.11 (t, *J* = 5.6 Hz, 1H, CH),

3.52 (s, 1H, SH), 1.67-1.51 (m, 2H, CH<sub>2</sub>) 1.31-1.21 (m, 4H, CH<sub>2</sub>) 0.83 (t,  $J = 5.2$  Hz, 3H, CH<sub>3</sub>). <sup>13</sup>C NMR (400 MHz, CDCl<sub>3</sub>)  $\delta$  13.9, 22.2, 27.3, 32.5, 43.5, 68.8, 114.4, 119.7, 130.2, 133.3, 148.1.



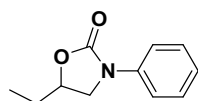
**Compound C7:**

<sup>1</sup>H NMR (400 MHz, DMSO-*d*<sub>6</sub>)  $\delta$  8.12 (s, 1H, ArH), 8.03 (s, 1H, ArH), 4.12 (dd,  $J = 3.2, 11.2$  Hz, 1H, CH), 3.98 (dd,  $J = 6.0, 11.2$  Hz, 1H, CH), 3.79 (m, 1H, CH), 1.39-1.33 (m, 2H, CH<sub>2</sub>) 1.32-1.21 (m, 4H, CH<sub>2</sub>) 0.83 (t,  $J = 5.6$  Hz, 3H, CH<sub>3</sub>). <sup>13</sup>C NMR (400 MHz, DMSO-*d*<sub>6</sub>)  $\delta$  13.9, 22.1, 27.2, 34.1, 49.1, 68.3, 118.5, 141.5, 149.7, 152.2, 155.9.



**Compound C9:**

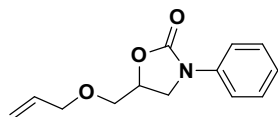
<sup>1</sup>H NMR (400 MHz, CDCl<sub>3</sub>)  $\delta$  7.53 (d,  $J = 6.4$  Hz, 2H, ArH), 7.37 (t,  $J = 5.6$  Hz, 2H, ArH), 7.11 (t,  $J = 5.6$  Hz, 1H, ArH), 4.79-4.76 (m, 1H, CH), 4.14 (t,  $J = 6.8$  Hz, 1H, CH), 3.65 (t,  $J = 6.4$  Hz, 1H, CH), 1.39 (d,  $J = 4.8$  Hz, 3H, CH<sub>3</sub>). <sup>13</sup>C NMR (400 MHz, CDCl<sub>3</sub>)  $\delta$  24.4, 54.7, 73.01, 120.2, 125.5, 130.9, 140.4, 155.8.



**Compound C10:**

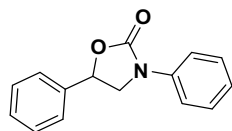
<sup>1</sup>H NMR (400 MHz, CDCl<sub>3</sub>)  $\delta$  7.44 (d,  $J = 6.4$  Hz, 2H, ArH), 7.27 (t,  $J = 6.0$  Hz, 2H, ArH), 6.96 (t,  $J = 5.6$  Hz, 1H, ArH), 4.74-4.69 (m, 1H, CH), 4.54 (t,  $J = 6.8$  Hz, 1H,

CH), 4.13 (t,  $J = 6.0$  Hz, 1H, CH), 1.68 (q,  $J = 5.2$  Hz, 2H, CH<sub>2</sub>), 0.89 (t,  $J = 5.6$  Hz, 3H, CH<sub>3</sub>). <sup>13</sup>C NMR (400 MHz, CDCl<sub>3</sub>)  $\delta$  8.4, 26.0, 68.9, 78.0, 118.2, 121.8, 128.8, 139.7, 152.6.



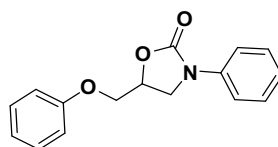
**Compound C11:**

<sup>1</sup>H NMR (400 MHz, CDCl<sub>3</sub>)  $\delta$  7.54 (d,  $J = 7.6$  Hz, 2H, ArH), 7.37 (t,  $J = 7.6$  Hz, 2H, ArH), 7.13 (t,  $J = 7.2$  Hz, 1H, ArH), 5.93-5.82 (m, 1H), 5.28 (d,  $J = 15.6$  Hz, 1H, CH), 5.21 (d,  $J = 10.4$  Hz, 1H, CH), 4.79-4.73 (m, 1H, CH), 4.06 (t,  $J = 7.4$  Hz, 3H), 3.94 (t,  $J = 7.4$  Hz, 1H), 3.69 (d,  $J = 4.8$  Hz, 2H). <sup>13</sup>C NMR (400 MHz, CDCl<sub>3</sub>)  $\delta$  47.2, 69.9, 71.2, 72.6, 118.1, 123.9, 128.9, 133.9, 138.2, 154.5.



**Compound C12:**

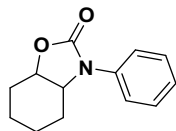
<sup>1</sup>H NMR (400 MHz, CDCl<sub>3</sub>)  $\delta$  7.54 (d,  $J = 8.0$  Hz, 2H, ArH), 7.41-7.35 (m, 7H, ArH), 7.13 (t,  $J = 7.6$  Hz, 1H, ArH), 5.66-5.59 (m, 1H), 4.77 (t,  $J = 8.8$  Hz, 1H, CH), 3.93 (t,  $J = 8.4$  Hz, 1H, CH). <sup>13</sup>C NMR (400 MHz, CDCl<sub>3</sub>)  $\delta$  52.6, 74.1, 118.3, 124.2, 125.7, 125.9, 129.1, 135.8, 138.1, 154.9.



**Compound C13:**

<sup>1</sup>H NMR (400 MHz, CDCl<sub>3</sub>)  $\delta$  7.58 (d,  $J = 6.8$  Hz, 2H, ArH), 7.39 (t,  $J = 6.0$  Hz, 2H, ArH), 7.29 (t,  $J = 6.0$  Hz, 2H, ArH), 7.13 (t,  $J = 6.0$  Hz, 1H, ArH), 6.96-6.94 (m, 3H,

ArH), 5.07-5.02 (m, 1H, CH), 4.29-4.28 (m, 1H, CH), 4.25-4.20 (m, 2H, CH<sub>2</sub>), 3.94-3.91 (m, 1H, CH). <sup>13</sup>C NMR (400 MHz, CDCl<sub>3</sub>) δ 46.3, 68.3, 70.8, 114.6, 117.9, 121.1, 123.5, 128.9, 129.5, 138.4, 154.1, 158.0.



**Compound C14:**

<sup>1</sup>H NMR (400 MHz, CDCl<sub>3</sub>) δ 7.39 (t, *J* = 7.2 Hz, 2H, ArH), 7.25 (d, *J* = 7.6 Hz, 2H, ArH), 7.21 (t, *J* = 7.6 Hz, 1H, ArH), 4.01 (t, *J* = 11.2 Hz, 1H, CH), 3.67 (t, *J* = 10.8 Hz, 1H, CH), 2.29-2.20 (m, 2H, CyCH), 1.99-1.88 (m, 2H, CyCH), 1.76-1.41 (m, 4H, CyCH). <sup>13</sup>C NMR (400 MHz, CDCl<sub>3</sub>) δ 23.59, 23.9, 28.2, 28.6, 63.9, 81.5, 122.9, 125.6, 129.0, 137.3, 157.7.

Section S4:  $^1\text{H}$  and  $^{13}\text{C}$  NMR spectra of oxazolidinones

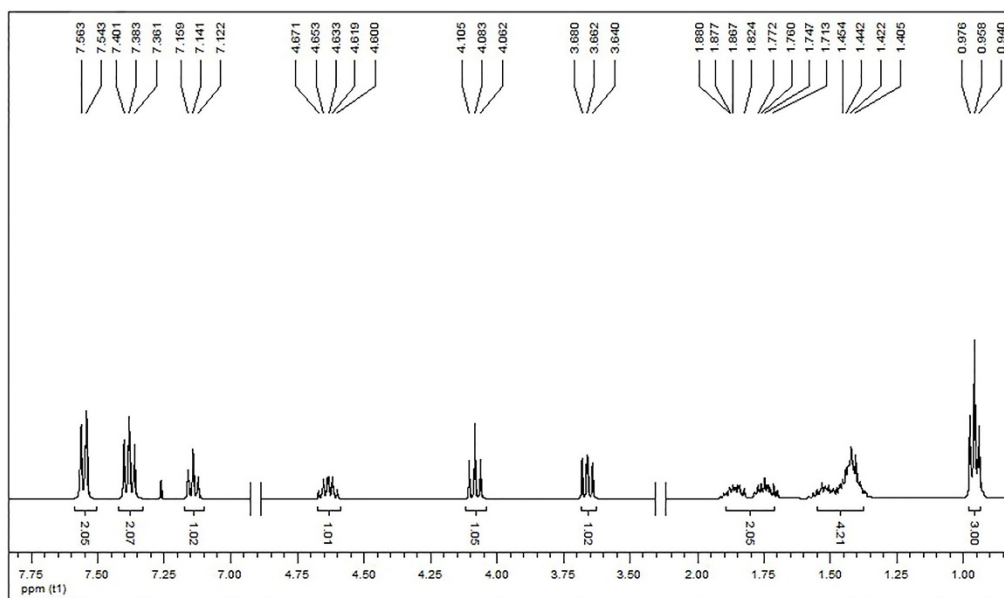
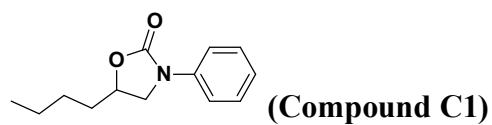


Figure S15:  $^1\text{H}$  NMR spectrum of C1 in  $\text{CDCl}_3$ .

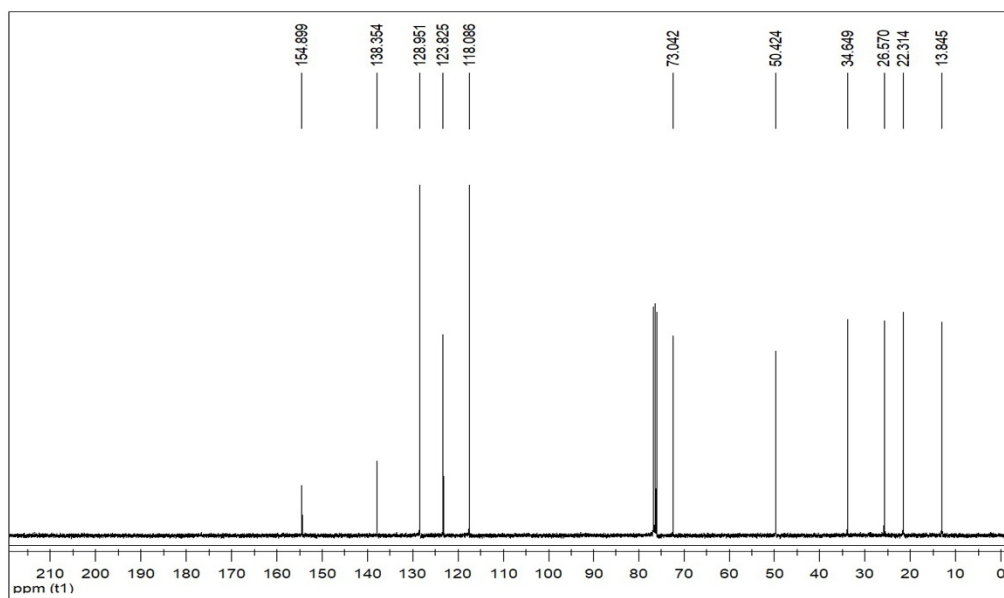


Figure S16:  $^{13}\text{C}$  NMR spectrum of C1 in  $\text{CDCl}_3$ .

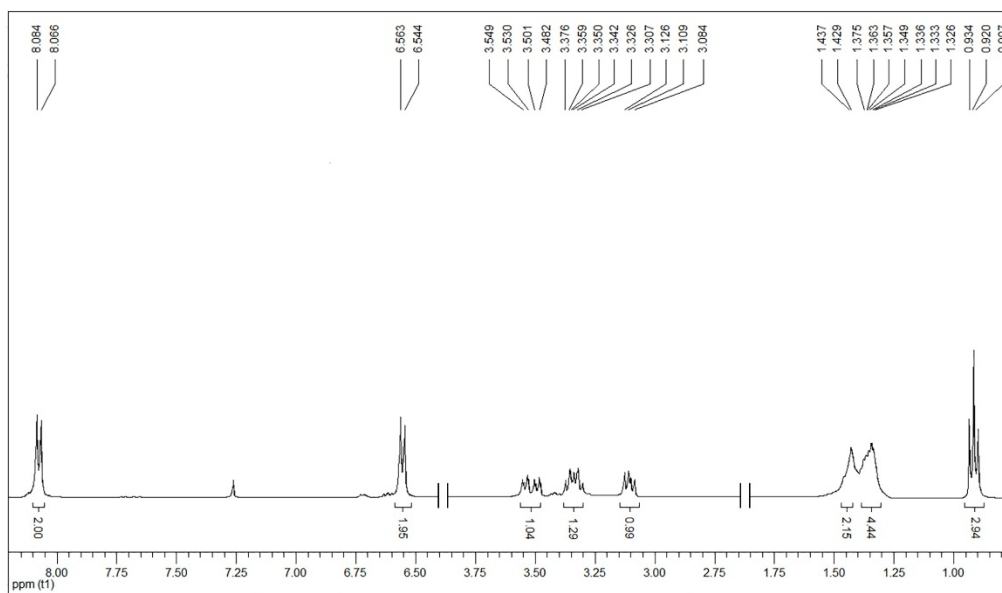
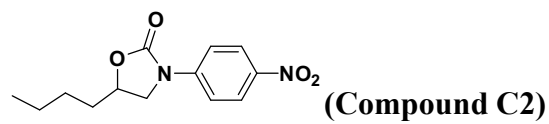


Figure S17:  $^1\text{H}$  NMR spectrum of C2 in  $\text{CDCl}_3$ .

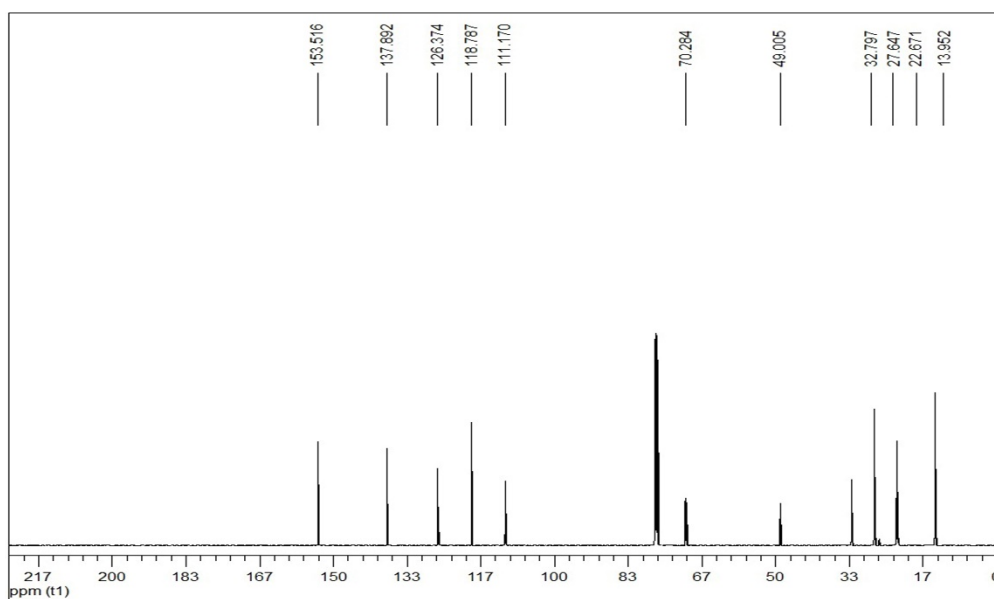
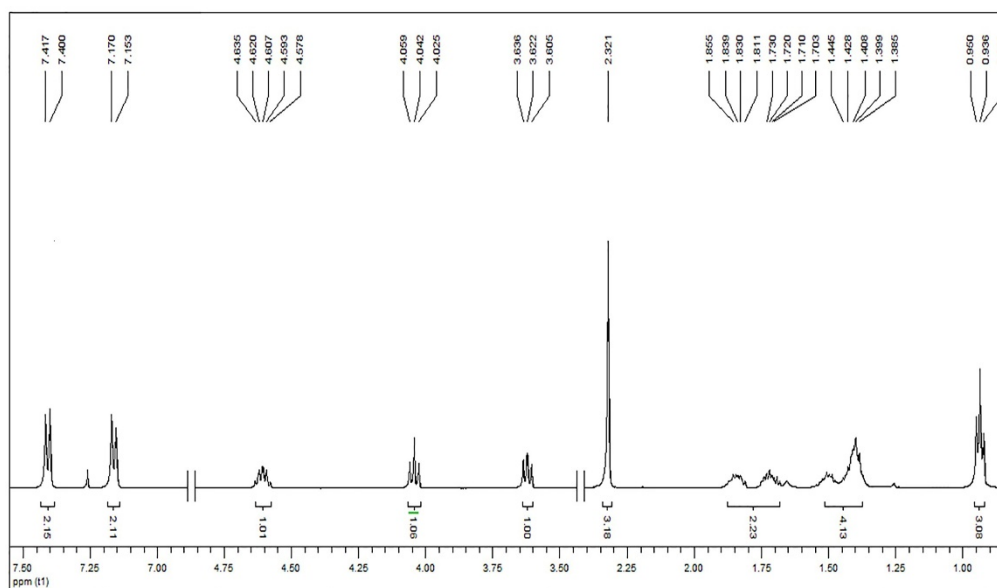
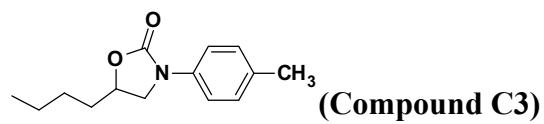
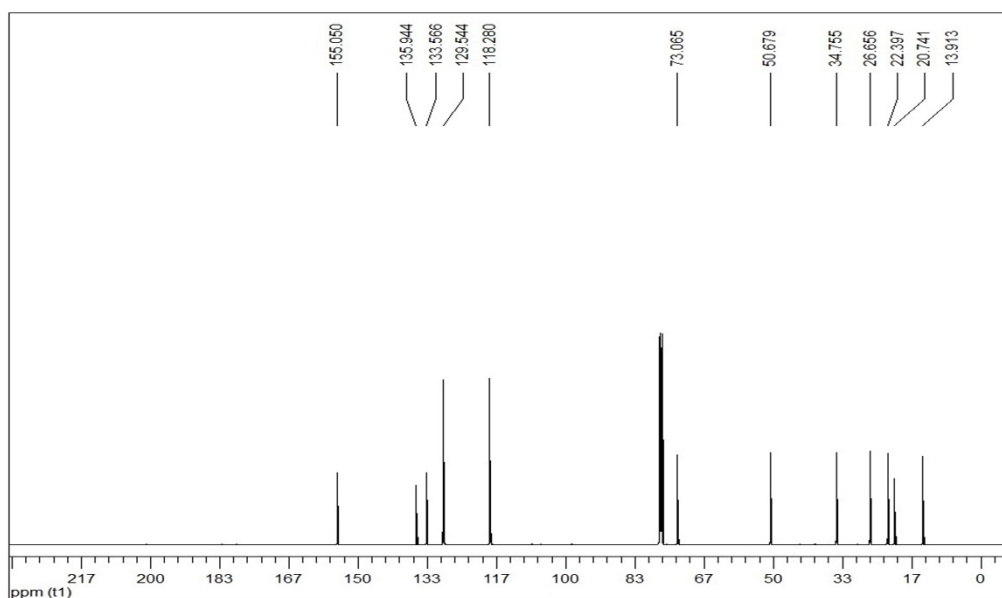


Figure S18:  $^{13}\text{C}$  NMR spectrum of C2 in  $\text{CDCl}_3$ .



**Figure S19:**  $^1\text{H}$  NMR spectrum of **C3** in  $\text{CDCl}_3$ .



**Figure S20:**  $^{13}\text{C}$  NMR spectrum of **C3** in  $\text{CDCl}_3$ .





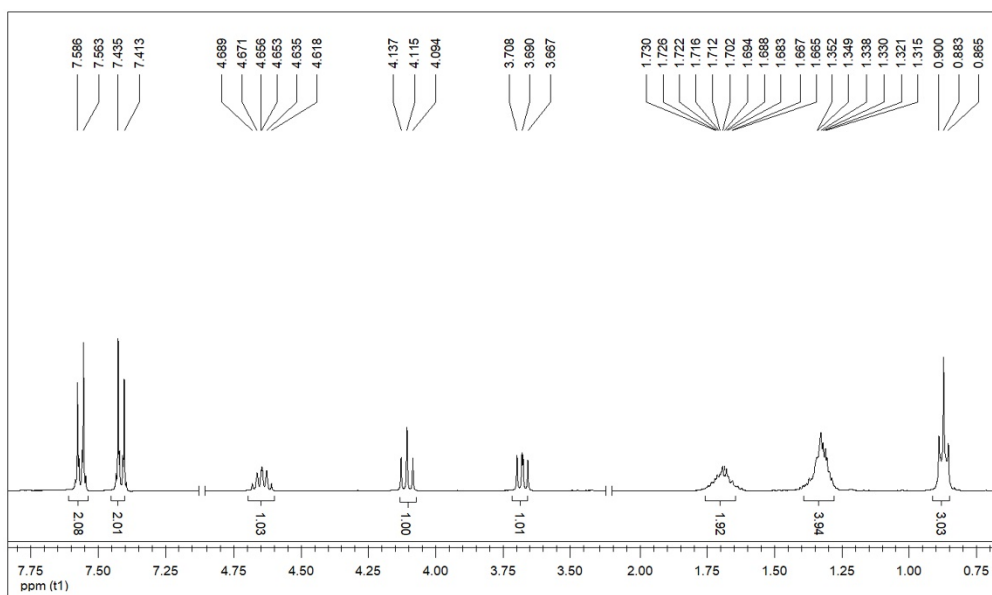
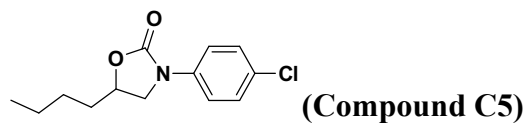


Figure S23:  $^1\text{H}$  NMR spectrum of C5 in  $\text{CDCl}_3$ .

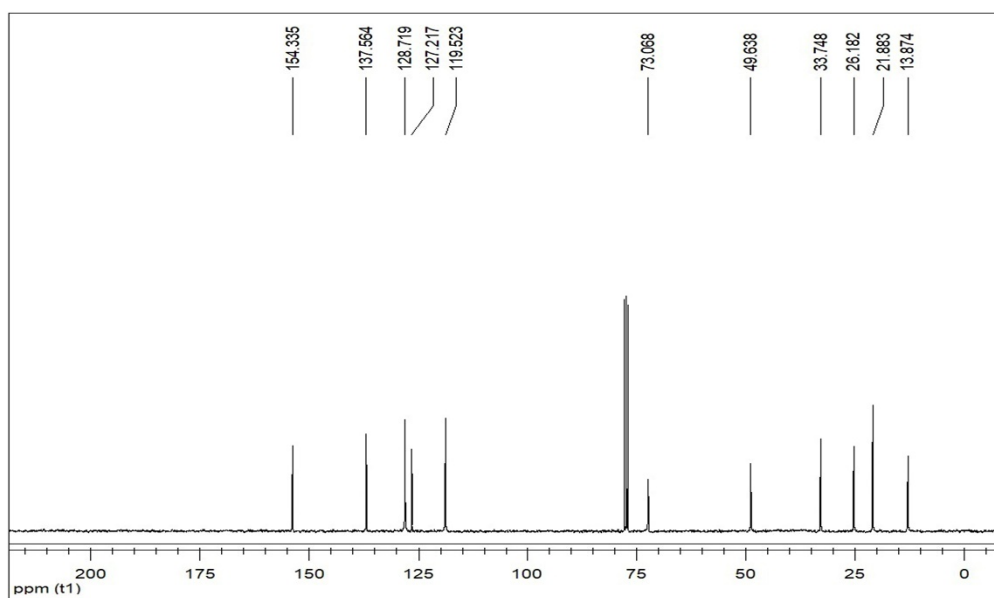


Figure S24:  $^{13}\text{C}$  NMR spectrum of C5 in  $\text{CDCl}_3$ .



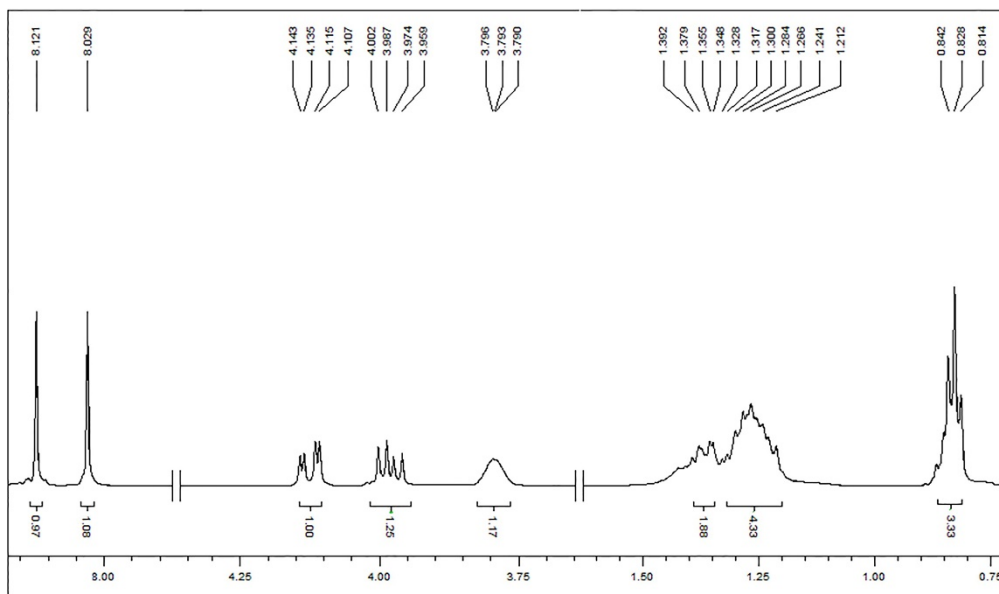
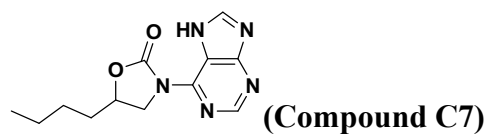


Figure S27:  $^1\text{H}$  NMR spectrum of C7 in  $\text{DMSO-}d_6$ .

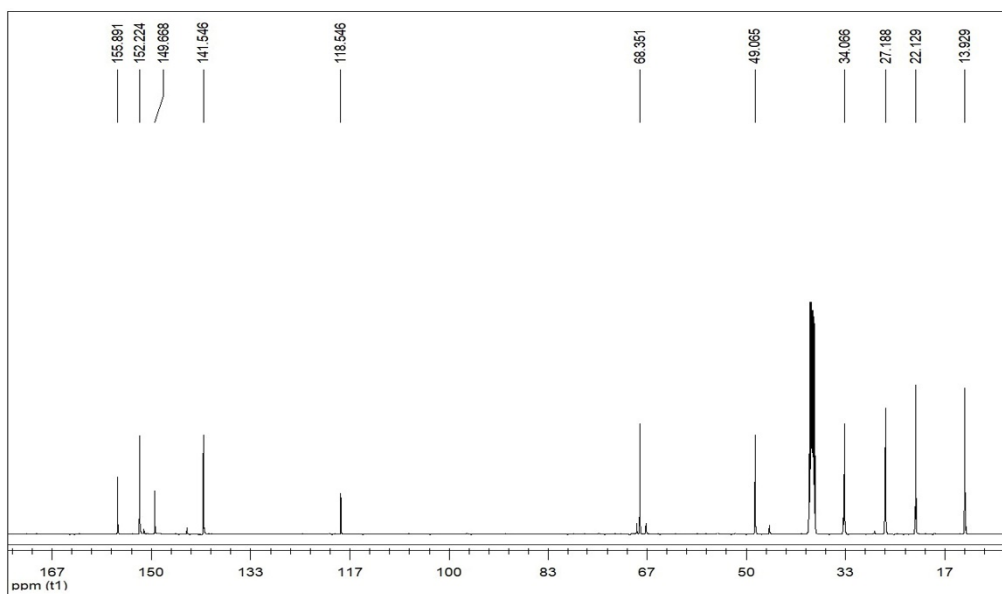


Figure S28:  $^{13}\text{C}$  NMR spectrum of C7 in  $\text{DMSO-}d_6$ .

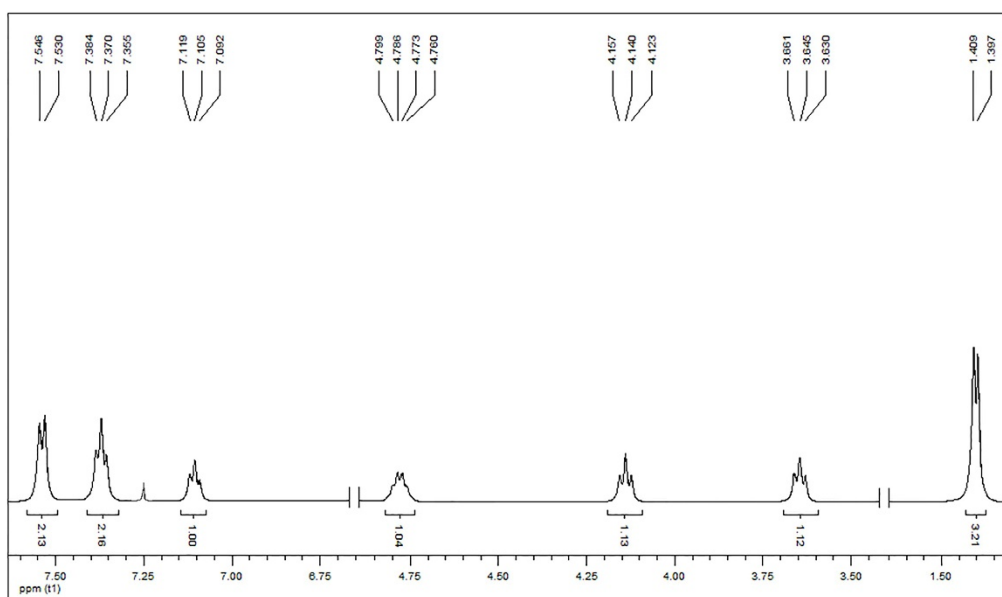
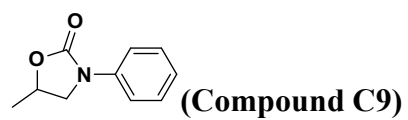


Figure S29: <sup>1</sup>H NMR spectrum of C9 in CDCl<sub>3</sub>.

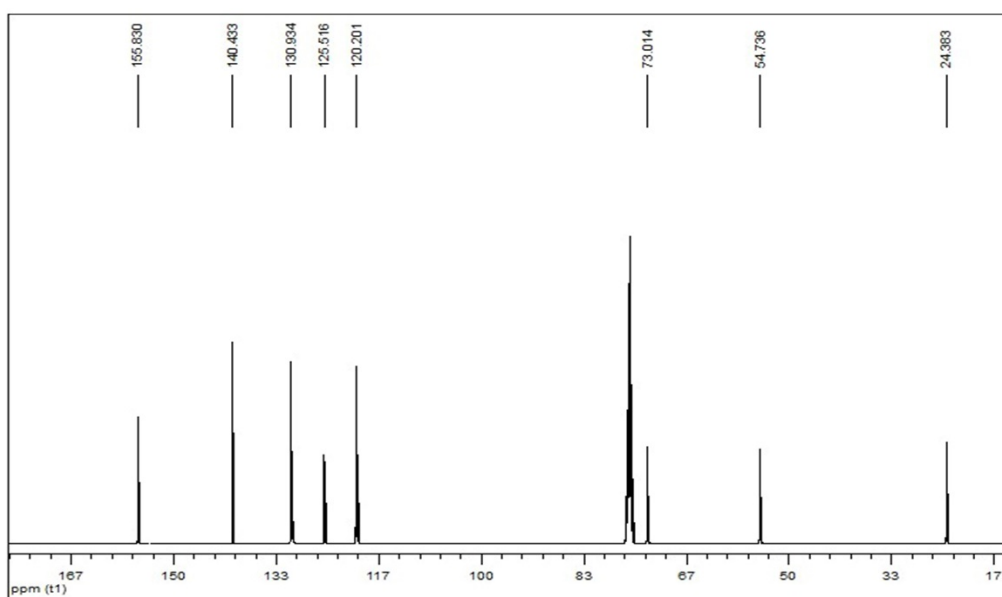


Figure S30: <sup>13</sup>C NMR spectrum of C9 in CDCl<sub>3</sub>.

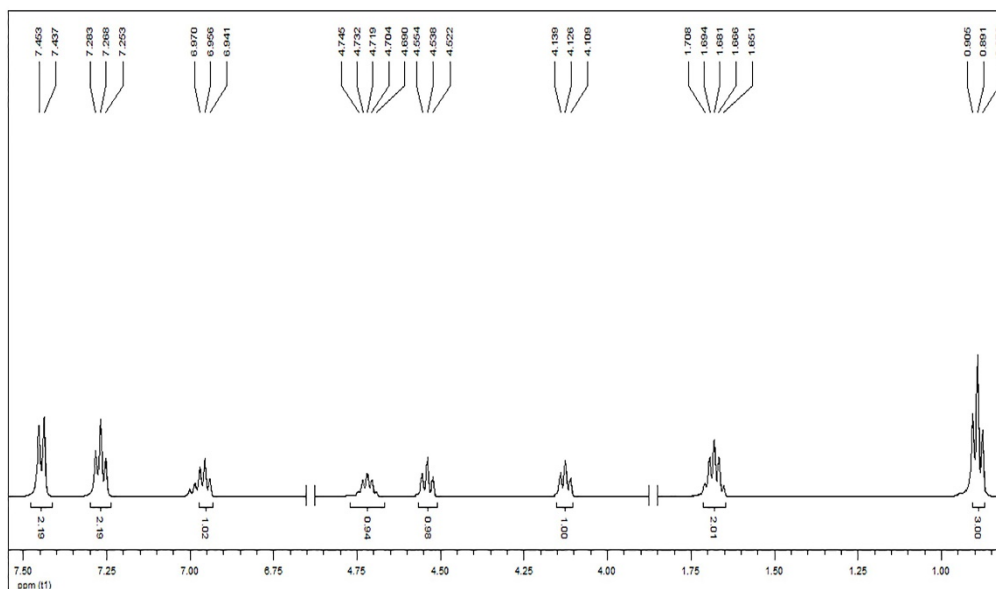
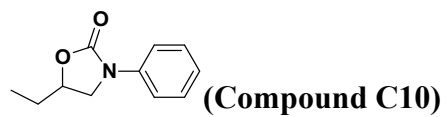


Figure S31:  $^1\text{H}$  NMR spectrum of C10 in  $\text{CDCl}_3$ .

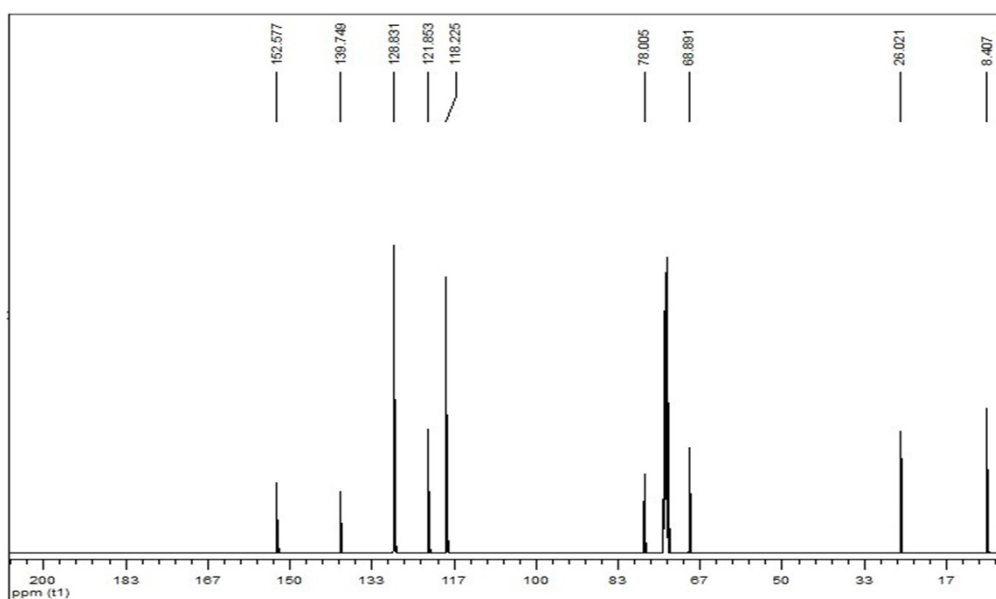


Figure S32:  $^{13}\text{C}$  NMR spectrum of C10 in  $\text{CDCl}_3$ .



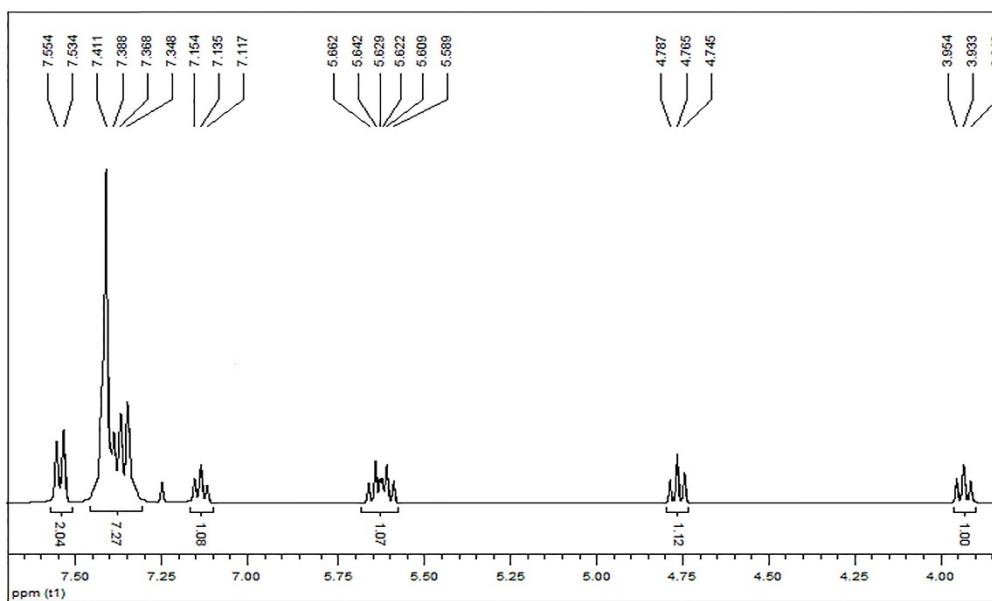
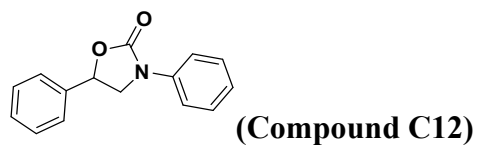


Figure S35:  $^1\text{H}$  NMR spectrum of C12 in  $\text{CDCl}_3$ .

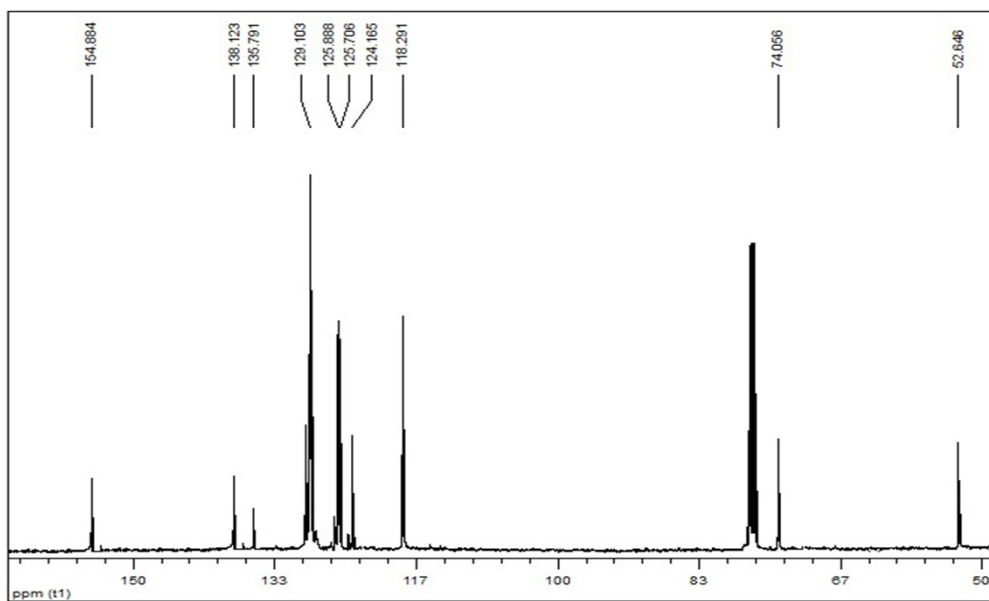
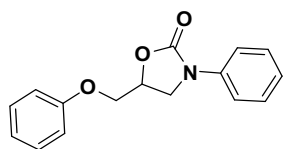


Figure S36:  $^{13}\text{C}$  NMR spectrum of C12 in  $\text{CDCl}_3$ .



(Compound C13)

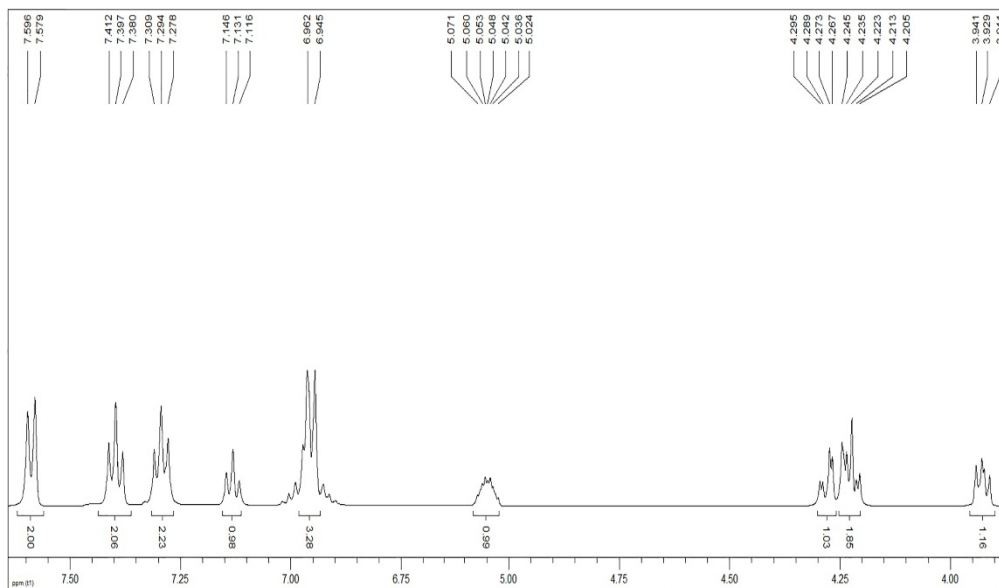


Figure S37:  $^1\text{H}$  NMR spectrum of C13 in  $\text{CDCl}_3$ .

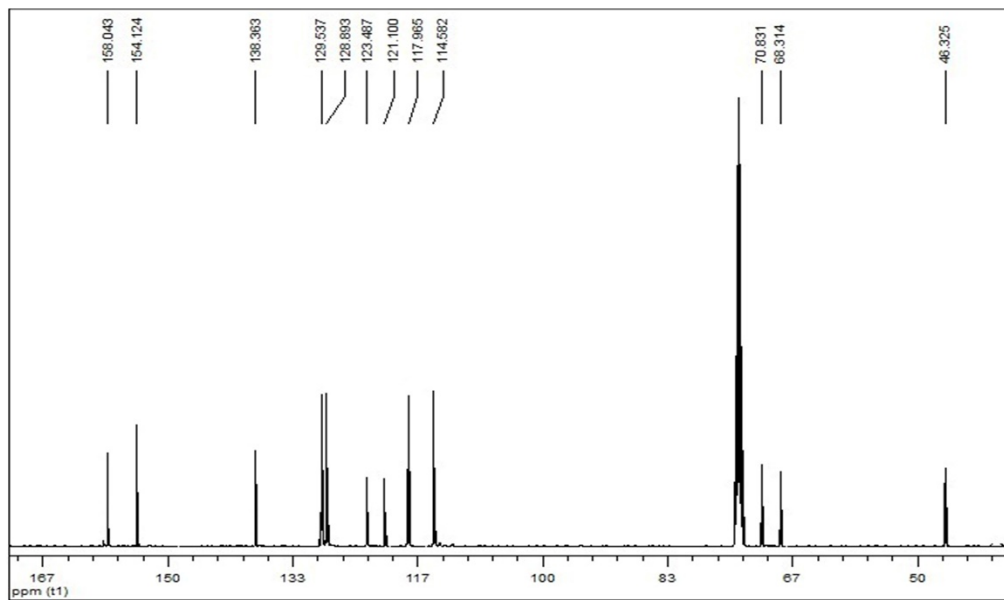
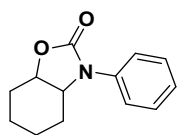


Figure S38:  $^{13}\text{C}$  NMR spectrum of C13 in  $\text{CDCl}_3$ .





(Compound C14)

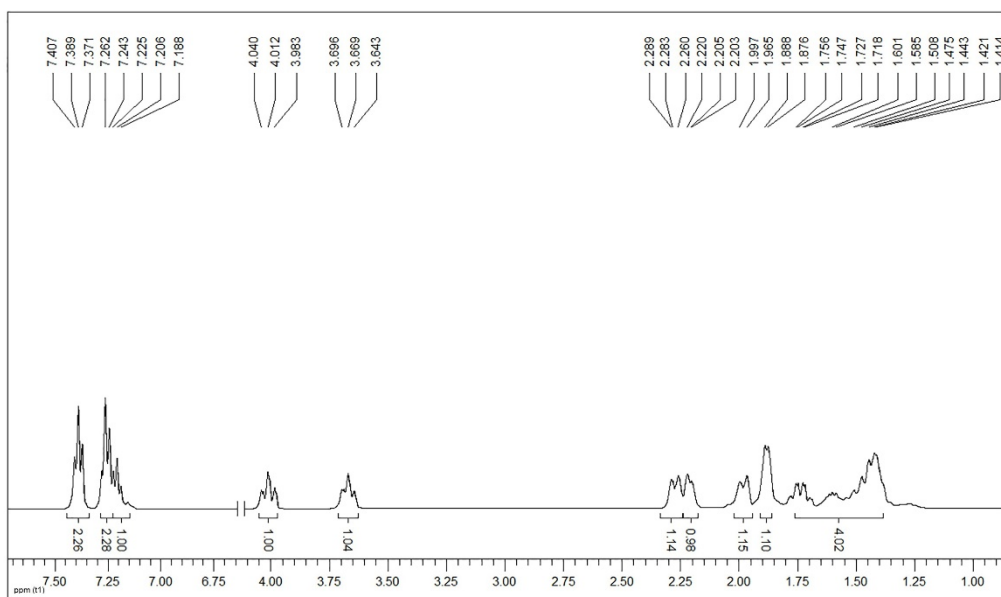


Figure S39: <sup>1</sup>H NMR spectrum of C14 in CDCl<sub>3</sub>.

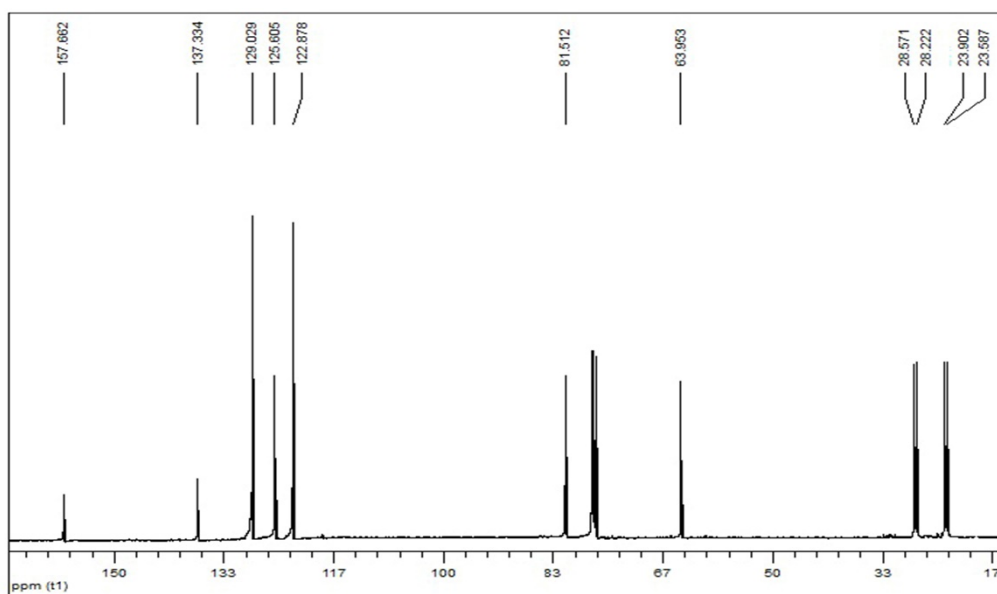
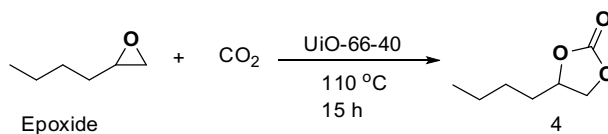


Figure S40: <sup>13</sup>C NMR spectrum of C14 in CDCl<sub>3</sub>.

## Section S5: Synthesis of the intermediates for the catalytic reaction



**Synthesis of 4:** 1,2-epoxy hexane (1.6 mL, 14 mmol), and UiO-66-40 (140 mg) were added into a 10 mL Schlenk flask attached with a balloon filled with CO<sub>2</sub>. The reaction mixture was heated at 110 °C for 15 h. The catalyst was separated by centrifugation with ethyl acetate three times. The combined ethyl acetate layer was concentrated and the product **4** was isolated by column chromatography (ethyl acetate/hexane 1:9) in yield of 40% (800 mg, 7.0 mmol).

<sup>1</sup>H NMR (400 MHz, CDCl<sub>3</sub>) δ 4.73-4.69 (m, 1H, CH), 4.55 (t, J = 9.2 Hz, 1H, CH<sub>2</sub>), 4.07 (dd, J = 8.0, 5.2 Hz, 1H, CH<sub>2</sub>), 1.57-1.52 (m, 2H, CH<sub>2</sub>), 1.47-1.35 (m, 4H, CH<sub>2</sub>), 0.92 (t, J = 7.2 Hz, 3H, CH<sub>3</sub>).

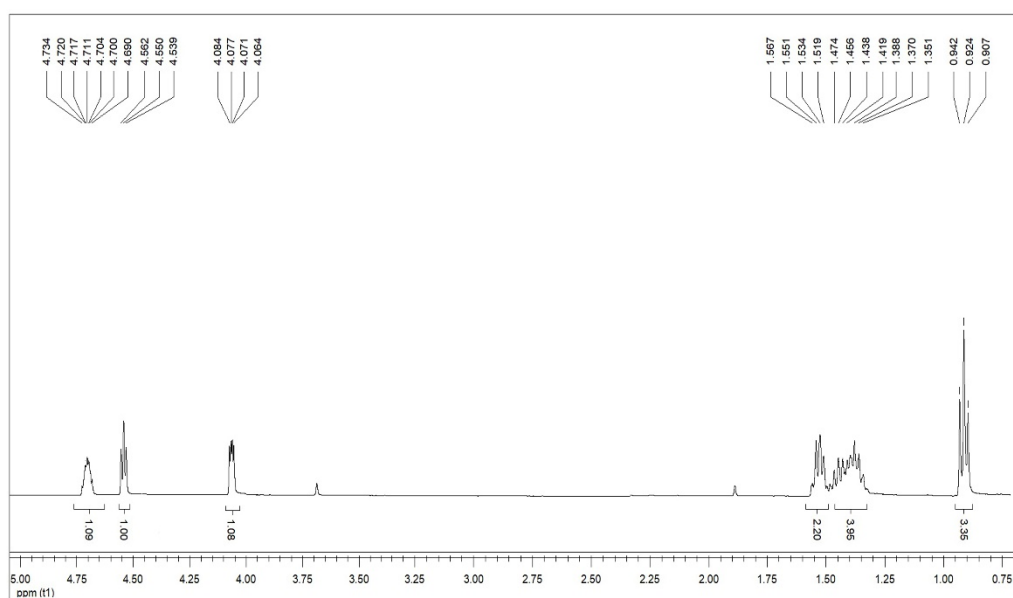
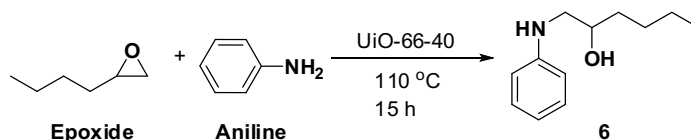


**Figure S41:** <sup>1</sup>H NMR spectrum of intermediate **4** in CDCl<sub>3</sub>.



**Synthesis of 6:** 1,2-epoxy hexane (3.1 mL, 27 mmol), aniline (0.5 mL, 5.4 mmol), and UiO-66-40 (140 mg) were added into a 10 mL Schlenk flask. The reaction mixture was heated at 110 °C for 15 h. The catalyst was separated by centrifugation with ethyl acetate three times. The combined ethyl acetate layer was concentrated and the product **6** was isolated by column chromatography (ethyl acetate/hexane 1:4) in yield of 25% (261 mg, 1.35 mmol).

$^1\text{H}$  NMR (400 MHz,  $\text{CDCl}_3$ )  $\delta$  7.38 (t,  $J = 7.6$  Hz, 2H, ArH), 7.14 (t,  $J = 7.2$  Hz, 1H, ArH), 6.65 (d,  $J = 8.0$  Hz, 2H, ArH), 3.60-3.56 (m, 1H, CH), 3.29 (dd,  $J = 18.8, 3.2$  Hz, 1H,  $\text{CH}_2$ ), 3.12 (dd,  $J = 10.8, 3.6$  Hz, 1H,  $\text{CH}_2$ ), 1.69-1.51 (m, 2H,  $\text{CH}_2$ ), 1.44-1.29 (m, 4H,  $\text{CH}_2$ ), 0.94 (t,  $J = 7.2$  Hz, 3H,  $\text{CH}_3$ ).

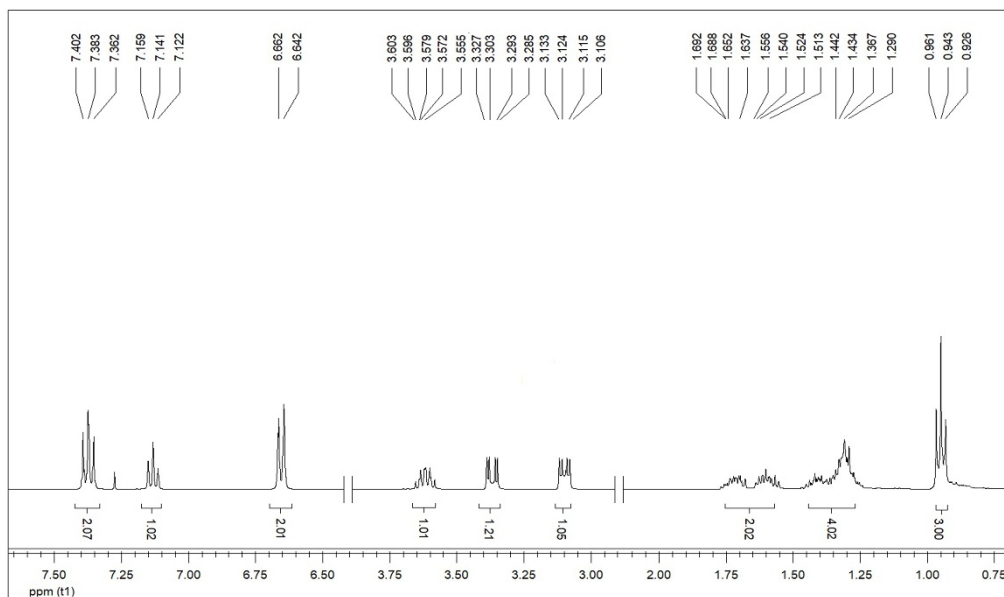
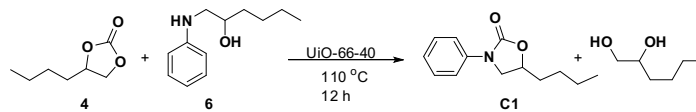


**Figure S42:**  $^1\text{H}$  NMR spectrum of intermediate **6** in  $\text{CDCl}_3$ .



**Synthesis of C1 from intermediates 4 and 6:** Intermediate 4 (720 mg, 5 mmol), intermediate 6 (400 mg, 2 mmol), and UiO-66-40 (70 mg) were added into a 10 mL Schlenk flask. The reaction mixture was heated at 110 °C for 12 h. The catalyst was separated by centrifugation with ethyl acetate three times. The combined ethyl acetate layer was concentrated and the product **C1** was isolated by column chromatography (ethyl acetate/hexane 1:4) in yield of 65%.

## Section S6: Recycling and regeneration of the catalyst UiO-66-40

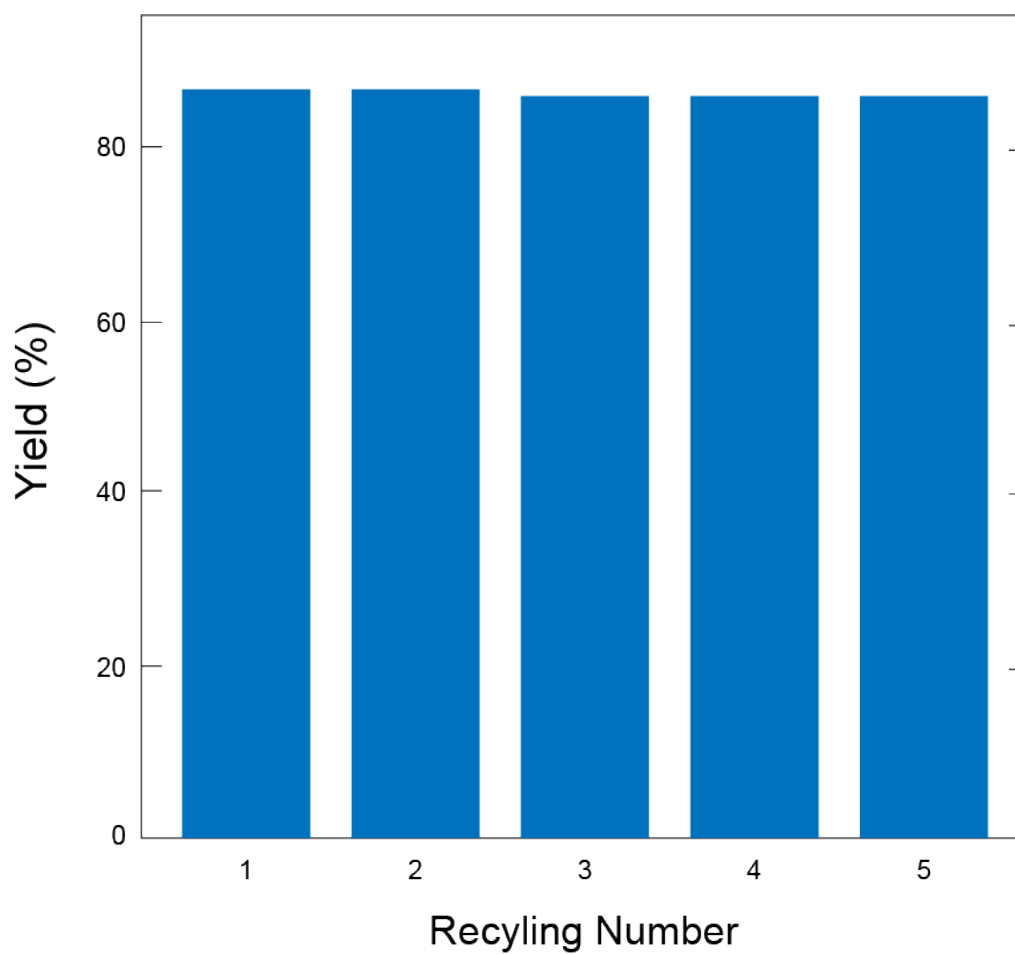


**Figure S43:** Recycle tests with UiO-66-40 for the reaction of CO<sub>2</sub> with aniline and 1,2-epoxyhexane to form oxazolidinone.

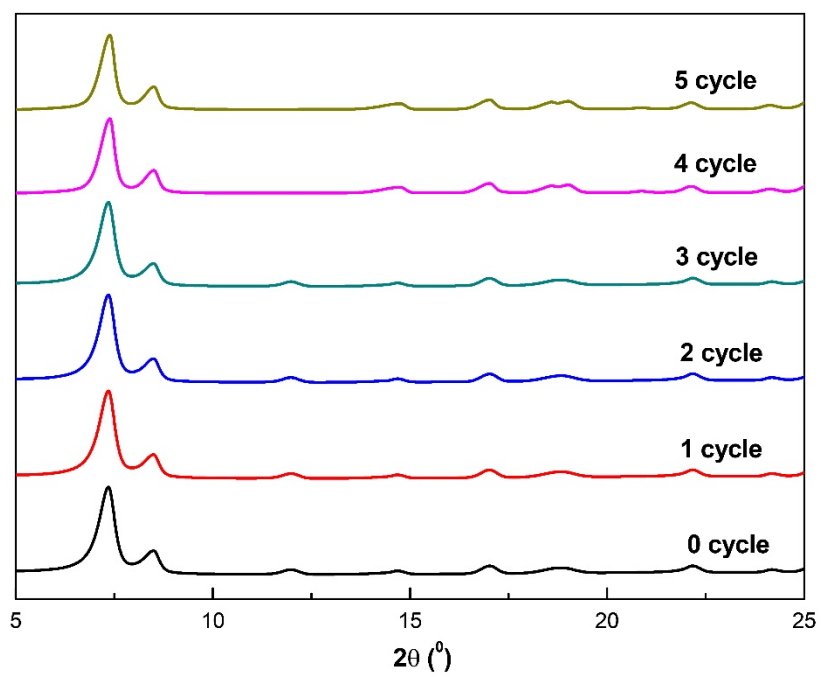


**Figure S44:** PXRD of the catalyst UiO-66-40 recovered after each cycle.

## Section S7: References

1. Choi, K. M.; Na, K.; Somorjai, G. A.; Yaghi, O. M. *J. Am. Chem. Soc.* **2015**, *137*, 7810–7816.
2. Seo, U. R.; Chung, Y. K. *Green Chem.* **2017**, *19*, 803.
3. Lv, M.; Wang, P.; Yuan, D.; Yao, Y. *Chem. Cat. Chem.* **2017**, *9*, 4451.